Pion Superradiant Instabilities of Primordial Black Holes

Paulo Bernardo Figueira da Silva Ferraz
Mestrado em Física (Especialização Teórica)
Departamento de Física e Astronomia
2019

Orientador
Dr. João Pedro Trancoso Gomes Rosa, Investigador Auxiliar, Departamento de Física, Universidade de Aveiro

Coorientador
Prof. Orfeu Bertolami, Professor Catedrático, Departamento de Física e Astronomia, Faculdade de Ciências, Universidade do Porto

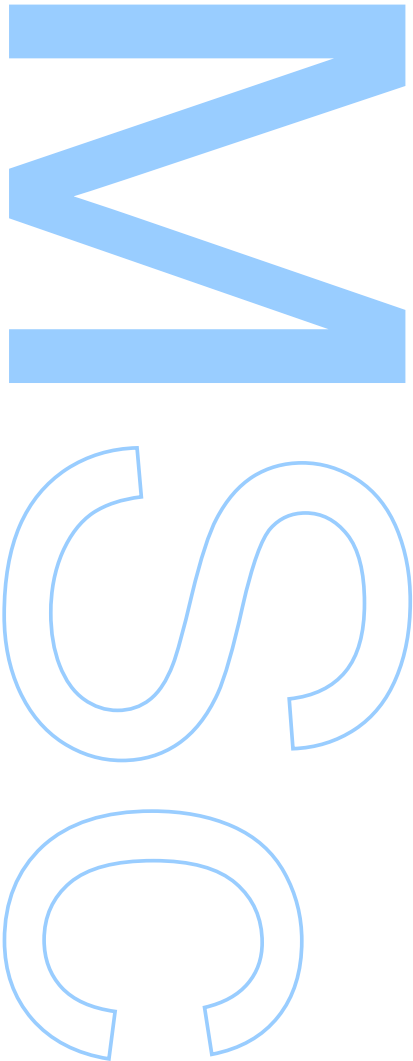

U.PORTO

FACULDADE DE CIÊNCIAS
UNIVERSIDADE DO PORTO

Todas as correções determinadas pelo júri, e só essas, foram efetuadas.

O Presidente do Júri,

Porto, _____/_____/_____

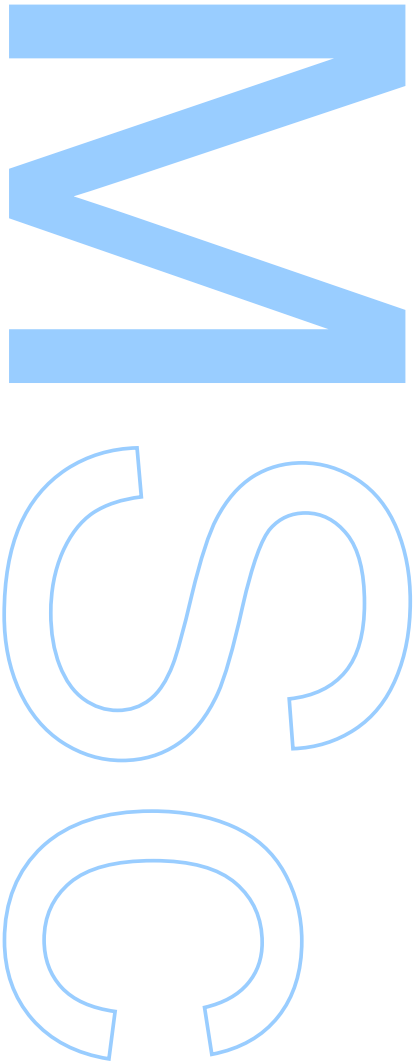

UNIVERSIDADE DO PORTO

MASTER THESIS

Pion Superradiant Instabilities of Primordial Black Holes

Author:
Paulo Bernardo Figueira da Silva Ferraz

Supervisor:
Dr. João G. Rosa

Co-supervisor:
Prof. Orfeu Bertolami

A thesis submitted in fulfilment of the requirements
for the degree of Master in Science

at the

Faculdade de Ciências
Departamento de Física e Astronomia

November 2019

" ...but you know the more one does the more one can do."

Amelia Earhart

Acknowledgements

Em primeiro lugar, gostaria de agradecer à pessoa que esteve comigo na linha da frente deste projeto, o meu orientador Professor João Rosa, por todo o conhecimento que me transmitiu e por toda a ajuda que me deu. O seu interesse e gosto pelos problemas atuais na física, e na ciência em geral, é contagiante e, pelo facto, de ter tido a oportunidade de estudar diversos tópicos sob a sua orientação foi deveras gratificante e fascinante. Portanto, um muito obrigado por toda a atenção e disponibilidade oferecidas.

Gostaria de agradecer ao meu co-orientador Professor Orfeu Bertolami por tornar este projeto possível. Aos professores e alunos da Universidade de Aveiro, com quem tive o prazer de trocar ideias dentro e fora do *journal club*, um obrigado por me acolherem de uma forma tão aberta e simpática.

Também gostava de agradecer ao Dr. Thomas Kephart pela sua revisão e sugestões perante este trabalho.

Por toda a força e incentivo diário, um obrigado à minha querida mãe Susana. Também um agradecimento para toda a minha família pelo interesse que demonstraram no meu trajeto académico. Com uma especial menção ao meu avô Humberto e que descanse com a paz que merece.

Aos meus amigos, um obrigado pelos cafés e pelas sessões de *bodyboard* que tanto me ajudaram a refrescar ideias.

UNIVERSIDADE DO PORTO

Abstract

Faculdade de Ciências
Departamento de Física e Astronomia

Master in Science

Pion Superradiant Instabilities of Primordial Black Holes

by Paulo Bernardo Figueira da Silva Ferraz

The study of the superradiance phenomenon is a crucial part to understand the physics of black holes and to probe high energy physics. We present a review of black holes in General Relativity (GR), emphasizing their most notable characteristics. Following this review, an analysis of the Kerr black hole is made in such detail that the study of the dynamics of a massive bosonic field is possible. The presence of a massive bosonic field in a Kerr spacetime leads to superradiant instabilities of the particles associated with the field and the solutions associated with these superradiant instabilities can have a complex structure such that analytical solutions are only possible in certain conditions. We make an extention of the analytical solution of the fastest superradiant mode growth rate of a spin-0 field. This extention is in agreement with the numerical results with an average error $\lesssim 50\%$. The main objective of obtaining such a result is to have an analytical expression such that it gives, at least, the correct order of magnitude of the growth rate. We proceed by studying the dynamics and phenomenology associated with pions under the influence of superradiant instabilities in which a pion cloud with a nuclear density is formed around the black hole. The black holes that can produce pion superradiant instabilities have a mass corresponding to the mass of black holes formed in the early universe, i.e. primordial black holes. From the decay and annihilation of pions into photons, we compute the net photon flux generated by the cloud and comparate it with observational data. We conclude that the obtained constraints are comparable with the already existing from Hawking evaporation in the corresponding mass range. We also present some observational prospects of such phenomena.

UNIVERSIDADE DO PORTO

Resumo

Faculdade de Ciências
Departamento de Física e Astronomia

Mestre em Ciência

Instabilidades superradiantes de Piões em Buracos Negros Primordiais

por Paulo Bernardo Figueira da Silva Ferraz

O estudo do fenómeno de superradiância é uma parte fundamental para compreender a física de buracos negros e para testar a física de altas energias. Com isto, fazemos uma revisão de buracos negros em Relatividade Geral, em que apresentamos as suas principais características. De seguida, fazemos uma análise do buraco negro de Kerr, focando-nos no estudo da dinâmica de um campo bosónico massivo na vizinhança de um destes buracos negros. A presença de um tal campo num espaço-tempo de Kerr leva a que as particulas associadas a este campo sofram instabilidades superradiantes, em que as soluções associadas a este fenómeno têm uma estrutura complexa, daí que só haja soluções analíticas em certas condições. Focando-nos numa certa solução que irá corresponder ao modo do estado ligado com a taxa de produção mais elevada associada a um campo escalar, é apresentada uma extensão desta solução analítica tal que os seus valores estejam em concordância com os valores numéricos. Esta extensão não tem como objetivo obter resultados com elevada precisão mas que dê, pelo menos, a ordem de magnitude correta, daí que impusemos que o erro relativo médio seja menor ou igual a 50%. Dá-se uma continuação ao trabalho estudando a dinâmica e fenomonologia associada a piões que estejam sob a influência de instabilidades superradiantes em que, por consequência, estarão presentes como estados ligados numa nuvem com densidade nuclear em volta do buraco negro. Os buracos negros que estão associados a estas instabilidades superradiantes em piões serão buracos negros formados no início do universo, conhecidos como buracos negros primordiais. Através do decaimento e aniquilação de piões em fotões, fazemos uma comparação entre o fluxo de fotões resultante e o fluxo de fotões observado no fundo extragaláctico de raios gama. Concluimos que os constragimentos obtidos são comparáveis com os constragimentos já existentes associados à evaporação de Hawking na correspondente gama de massas. No final, apresentamos algumas perspectivas observationais deste fenómeno.

Contents

List of Figures

Notation and Conventions

Through out this work we use natural units $\hbar = c = G = 1$ unless otherwise mentioned.

We use as signature $(-+++)$ for the metric and $\eta_{\mu\nu}$ corresponds to the Minkowski metric and $g_{\mu\nu}$ to non-Minkowski metrics.

In the legends of some plots, we use the notation $M = M_{11} \times 10^{11}$ kg.

Abbreviations

BH	**B**lack **H**ole
PBH	**P**rimordial **B**lack **H**ole
GR	**G**eneral **R**elativity
QCD	**Q**uantum **C**hromo**D**ynamics
QED	**Q**uantum **E**letro**D**ynamics
EM	**E**letro**M**agnetism
SRA	**S**low-**R**oll **A**pproximation
CMB	**C**osmic **M**icrowave **B**ackground

Chapter 1

Motivation and Objectives

When Albert Einstein presented one of the pilars of modern physics, the Theory of General Relativity (GR), with it came a new whole spectrum of peculiarities. One of the peculiarities is the prediction of objects whose gravitational fields are so strong that nothing can escape from it, not even light. These objects would be baptized as Black Holes (BH). The first type of BH was proposed by Karl Schwarzchild, an object which satisfies the Einstein Field Equations (EFE) for an empty spherical symmetric spacetime. One of the most remarkable characteristics of this object was the existence of a surface that functions as a one-way membrane, known as *event horizon*. After this solution, another one was discovered which describes rotating black holes. The Kerr solution aside from possessing an event horizon, would also contain a region where processes of radiation enhancement are possible and this region is known as ergoregion. One of this processes includes the Penrose process, where if a particle decays into two others inside the ergoregion, while one of the particles falls into the black hole, the other can escape to outside of the ergoregion and arise with an energy greater than the original particle. An analogous phenomenon which occurs if we consider the scattering of waves into the black hole is known as superradiance [3].

Considering a black hole with angular velocity Ω_H at the horizon and a scattered wave of frequency ω, superradiance can occur if $\omega < m\Omega_H$, where m is the azimuthal quantum number along the axis of rotation. The wave can be reflected back by the black hole while being amplified. Substituting the concept of a wave with a massive bosonic field in the vicinity of a Kerr black hole, with frequency satisfying the previous condition, a cloud of particles that are copiously produced in quasi-bound states can be generated around the black hole at the expense of its rotational energy. The concept of superradiance was originated in the works of Klein when studying the Dirac equation in the presence of a potential barrier and in the work of Zel'dovich showing that an absorbing rotating cylinder could amplify an incident wave if its frequency was bound by a multiple of the angular velocity of the cylinder.

Shortly after the prediction of black holes, it was thought that the only way that these objects could be formed was from the collapse in the final stages of an old star. Zel'dovich and Novikov [4] presented a new possibility in which black holes could be formed and later a more detailed analysis was made by Stephen Hawking [5] and also by Bernard Carr [6]. Black holes could be generated due to the fluctuations of the primeval universe. While black holes originating from the collapse of stars have a typical mass of the order of the sun's mass $M_\odot$, these black holes could have a mass between a naive 10^{-5} g and an enormous $10^5 M_\odot$. These black holes would be later known as Primordial Black Holes (PBH). Already with the idea of superradiance and the possible smallness associated with a black hole mass, Hawking proceeded in studying the quantum properties of such black holes and made the magnificent discovery that a black hole can emit thermal radiation [7]. This was one of the first steps to conjugate different areas of physics such as General Relativity, Quantum Mechanics and Thermodynamics. This phenomenon would dictate the black hole lifetime and black holes with a mass $M \lesssim 1 \times 10^{12}$ kg would have evaporated by the present epoch.

Black holes have been considered as great laboratories to probe high energy physics due to superradiance [8, 9]. The effects of superradiance are more relevant when the mass of the black hole, M, and the mass of the field, μ, are correlated as $M\mu \sim 1$. One of the main focus in particle physics is the study of the Quantum Chromodynamics (QCD) axion, which was postulated to explain the strong CP problem [10]. The mass of the axion can be such that the correspondent black hole mass relevant for superradiance is associated with astrophysical black holes, i.e. masses of the order of the Sun. Presently, there has been great interest in astronomy directed to black hole observations and since the axion can have influence in the dynamics of a black hole when under the influence of superradiant instabilities, its effects can affect observations. Conversely, particle physics can also be used to study the properties of black holes and that is the main objective of this work. We will use as test particles pions, both neutral and charged. Their masses are similar, $\mu_0 \approx \mu_+$, and the correspondent black hole masses that can lead to superradiant instabilities are indicative of primordial black holes. Through their decay and annihilation into photons, we study in which conditions pion superradiant instabilities are permitted and comparing the associated net flux of photons with the observed extragalactic gamma ray background [11–14] we compute which fraction of dark matter can be in primordial black holes, constraining their mass and spin.

The outline of the work is the following:

In chapter 2, we present a brief review of black holes in General Relativity, demonstrating the existence of an event horizon and of thermal radiation (Hawking radiation). Then, we make a more extensive introduction to the Kerr black hole, showing some of its properties as singularities, isometries and angular velocity, followed by the description of the ergoregion and the Penrose process. In the following section we discuss the early signs of superradiance

in the Klein Gordon paradox which will be the follow up to superradiant instabilities. In the section of superradiant instabilities we derive all the formalism behind it, always focusing on a spin-0 field. In particular, we obtain a novel analytical expression for the growth rate of the superradiant instability in the leading mode that is a good fit to numerical results. The chapter ends with a discussion of the complementarity between particle physics and superradiance.

In chapter 3, we discuss some properties of pions, mainly we start with the quark model to explain the composition of hadrons. Then, we make a brief revision of the QCD formalism such that we arrive to an Effective Field Theory (EFT) that describes pions at low energies. We then use these two results to explain some characteristics of the pion, emphasizing its decay into photons and correspondents decay rates.

In chapter 4, we discuss primordial black holes. We present some formation mechanisms due to primordial fluctuations of the inflaton field in the early universe, and discuss their possible masses and spins. In the last section we show the observational constraints on the mass of these black holes.

In chapter 5, we study in which conditions pion superradiant instabilities are possible. Evaluating the dynamics of a black hole that produces such superradiant instabilities, we compute the duration of the superradiant energy extraction. The decay and annihilation of pions, during this period, results in a net flux of photons and, comparing this flux with the extragalactic $\gamma-$ray background, we put constraints on the mass and spin of such black holes. We also consider a point source at high redshift containing a large number of superradiant primordial black holes and evaluate the prospects for observing the photons from pion decay and annihilation.

Chapter 2

Black Hole Superradiance

This chapter serves as a brief review of black holes in General Relativity, pointing out which kind of black holes there are and their most notable characteristics using the Schwarzschild case to demonstrate them. Then, a more extensive analyzies of the Kerr black hole is made such that it leads to a discussion of the black hole superradiance.

2.1 Black Holes in General Relativity

The revolutionary idea that Einstein brought to the table is that matter and geometry are coupled, i.e. matter can distort the space-time continnum, and this relationship is translated from his famous field equations,

$$R_{\mu\nu} - \frac{1}{2} g_{\mu\nu} R = 8\pi T_{\mu\nu}, \tag{2.1}$$

where $R_{\mu\nu}$ is the Ricci curvature tensor, $g_{\mu\nu}$ is the metric tensor, R is the Ricci scalar and $T_{\mu\nu}$ is the energy-momentum tensor. The set of partial differential equations (2.1), depending on the matter content and the structure of the space-time, may not have analytical solutions but in 1916, Karl Schwarzschild found the simplest exact solution, which represents the spherically symmetric empty space-time outside a spherically symmetric massive body [15]. This solution has been so important in the unfolding of the General Theory of Relativity due to the fact that most experiments to test the difference between GR and Newtonian theory are based on predictions of such solution.

2.1.1 Event Horizon

The metric can be given in Schwarzschild coordinates (t, r, θ, ϕ) [16] as

$$ds^2 = g_{\mu\nu}dx^\mu dx^\nu = -\left(1 - \frac{2M}{r}\right)dt^2 + \left(1 - \frac{2M}{r}\right)^{-1}dr^2 + r^2(d\theta^2 + \sin^2\theta d\phi^2). \tag{2.2}$$

The metric of Eq. (2.2) is valid for $r > 2M$ but it is interesting to see what happens if we consider the full range of values of r. At $r = 0$ and $r = 2M$ appears to exist, in each one of them, a singularity. If one computes an invariant coming from the curvature [17], it results in

$$I(r) = R^{ijkl}R_{ijkl} = \frac{48M^2}{r^6}. \tag{2.3}$$

For $r = 2M$ it takes a finite value, indicating that this might be a singularity due to a poor choice of coordinates. Defining the *Regge-Wheeler radial coordinate* r^*

$$r^* = r + 2M\ln\left|\frac{r - 2M}{2M}\right|, \tag{2.4}$$

and the ingoing radial null coordinate v

$$v = t + r^*, \tag{2.5}$$

the metric (2.2) can be rewritten with Eddington-Finkelstein coordinates (v, r, θ, ϕ) [16] as

$$ds^2 = -\left(1 - \frac{2M}{r}\right)dv^2 + 2drdv + r^2(d\theta^2 + \sin^2\theta d\phi^2). \tag{2.6}$$

The singularity at $r = 0$ remains but at $r = 2M$ the metric is still well-defined and thus this singularity disappeared. The interesting analyzis that can be made from Eq. (2.6) is that no future-directed timelike or null worldline coming from $r < 2M$ can reach the region $r > 2M$. This means that $r = 2M$ functions as a one-way membrane and it is called an *event horizon*. The existence of an event horizon is the most important property of a black hole, not only because it is what defines the very concept of black hole but because it makes possible the existence of certain phenomena such as Hawking radiation and superradiance.

In the initial space-time (M, g), where the metric g (2.2) defined by the Schwarzschild coordinates (t, r, θ, ϕ), one had to rule out the points $r = 0$ and $r = 2M$ since the metric is not well-defined there. Cutting out the surface $r = 2M$ divides the space-time into two disconnected components, $0 < r < 2M$ and $2M < r < \infty$ but one has to choose one component, being the obvious one $r > 2M$. But when changing Schwarzschild coordinates to Eddington-Finkelstein coordinates (v, r, θ, ϕ), the metric g' (2.6) is well-defined for $r = 2M$.

So the space-time M can be extended to a larger one M' since the region of (M', g') for which $0 < r < 2M$ is isometric, i.e. is equivalent, to the region of (M, g) for which $0 < r < 2M$ [17].

The event horizon is defined in the space-time manifold (M', g') as a null hypersurface, in which the vector normal to the hypersurface n is null, i.e. $n \cdot n = 0$. Besides being a null hypersurface, it is also a Killing horizon, in which the vector normal to the hypersurface is proportional to a *Killing vector*. Killing vectors are important because they are associated with the symmetries of the space-time and they satisfy $\nabla_\mu \xi_\nu + \nabla_\nu \xi_\mu = 0$. Studying the geodesics of the Killing field on the horizon, $\xi^\alpha \nabla_\alpha \xi^\mu = \kappa \xi^\mu$, one can obtain the *surface gravity* κ which is related with Hawking radiation. For the Schwarzschild case, $\kappa = \frac{1}{4M}$ [16].

2.1.2 Hawking Radiation

In 1975, Stephen Hawking discovered that BHs have a thermal emission and that the energy would be emitted at the expense of the black hole mass [7].

In the usual treatment of quantum field theory, one deals with flat spacetime and so when quantising a Hermitian scalar field, ϕ, that obeys the equation $\eta^{\mu\nu} \nabla_\mu \nabla_\nu \phi = 0$, one can decompose the field into positive and negative frequecy components,

$$\phi = \sum_j \left(v_j a_i + \overline{v}_j a_j^\dagger \right), \tag{2.7}$$

where v_i are a set of orthonormal solutions of the wave equation with only positive frequencies. The operators a_i and $a_i^\dagger$ are the usual annihilation and creation operators, respectively. The vaccum state can be defined as $a_i |0\rangle = 0$ for all i [7, 18–20].

When one introduces curvature, one can also consider a hermitian scalar field ϕ which obeys $g^{\mu\nu} \nabla_\mu \nabla_\nu \phi = 0$ but one cannot use the same treatment as in flat spacetime. This is due to the fact that positive and negative frequencies do not have an invariant meaning in curved space-time. If one has a spacetime with an initial flat region (1) which is followed by a region of curvature (2) finishing with a flat region (3), the initial base v_{1i} will not be the same as v_{3i}. Thus, considering that the initial vaccum is $|0_1\rangle$, it does not mean that this vaccum satisfies $a_{3i} |0_1\rangle = 0$, i.e. $|0_1\rangle \neq |0_3\rangle$. Since the spacetime associated with the process of gravitational collapse transforming into a black hole may not be everywhere stationary, the latter applies [7].

Defining, $t \to -\infty$ and $r \to \infty$ as the past null infinity, $\mathcal{F}^-$, and $t \to \infty$ and $r \to \infty$ as the future null infinity, $\mathcal{F}^+$, Hawking predicted that there should be a particle flux through $\mathcal{F}^+$ given a vaccum on $\mathcal{F}^-$ given by

$$< N_i >_{\mathcal{F}^+} = \frac{1}{e^{2\pi\omega_i/\kappa} - 1}, \tag{2.8}$$

which corresponds to the Planck distribuition of a black body radiation at the Hawking temperature

$$T_H = \frac{\hbar c^3}{8\pi M G k_B} \text{ K}. \tag{2.9}$$

for a Schwarzschild black hole. One conclude that the black hole radiates aways its energy at this temperature. Using Stephan's law, the luminosity of a black body is $L = \sigma A T^4$ with $\sigma \approx 5.67 \times 10^{-8}$ $\text{Wm}^{-2}\text{K}^{-4}$ and the "area" of the black hole event horizon $A = 16\pi(MG/c^2)^2$, the lifetime of the black hole is given by

$$\tau \approx 14 \times \left(\frac{M}{1.7 \times 10^{11}}\right) \text{ Gyr}. \tag{2.10}$$

Thus, black holes with a mass $M \lesssim 2 \times 10^{11}$ kg are evaporating today. In the following chapters, a more detailed analysis is considered.

2.2 Kerr black hole

2.2.1 General Characteristics

The Kerr black hole is a vaccum solution of the Einstein field equations for a stationary, axisymmetric and asymptotically flat spacetime. This solution is believed to describe the gravitational field outside a massive rotating body. In Boyer-Linquist coordinates, the metric takes the form

$$\begin{aligned} ds^2 = &-\frac{(\Delta - a^2\sin^2\theta)}{\Sigma}dt^2 - 2a\sin^2\theta\frac{(r^2 + a^2 - \Delta)}{\Sigma}dtd\phi + \\ &+\left(\frac{(r^2 + a^2)^2 - \Delta a^2 sin^2\theta}{\Sigma}\right)\sin^2\theta d\phi^2 + \frac{\Sigma}{\Delta}dr^2 + \Sigma d\theta^2, \end{aligned} \tag{2.11}$$

where $\Delta = r^2 - 2Mr + a^2$ and $\Sigma = r^2 + a^2\cos^2\theta$ [16]. M and a are constants, M representing the mass of the BH and $Ma = J$ the angular momentum of the BH as measured from infinity. One also define the dimensionless parameter $\tilde{a} = aM^{-1}$. It can be noticed that this solution has the isometry $t \to -t, \phi \to -\phi$ but not $t \to -t$ alone, which make sense since time inversion of a rotating object produces another object rotating in the opposite direction [17]. Also, if one takes the limit $a \to 0$, it reduces to the Schwarzschild solution.

In these coordinates, the Kerr metric has as coordinate singularities $\theta = 0$ and $\Delta = 0$, in which $\Delta = (r - r_+)(r - r_-)$ for $r_\pm = M \pm \sqrt{M^2 - a^2}$. It also has a curvature singularity at $\Sigma = 0$, i.e. $r = 0$ and $\theta = \frac{\pi}{2}$. If one makes the change of coordinates to Kerr-Schild coordinates defined by

$$x + iy = (r + ia)\sin\theta e^{i\int(d\phi + \frac{a}{\Delta}dr)}, \tag{2.12}$$

$$z = r\cos\theta, \tag{2.13}$$

$$\tilde{t} = \int\left(dt + \frac{r^2 + a^2}{\Delta}dr\right) - r, \tag{2.14}$$

which implies that $r = r(x, y, z)$ is given implicity by

$$r^4 - (x^2 + y^2 + z^2 - a^2)r^2 - a^2z^2 = 0, \tag{2.15}$$

the metric (2.11) can be rewritten as [16]

$$\begin{aligned} ds^2 = &-d\tilde{t}^2 + dx^2 + dy^2 + dz^2 + \\ &+\frac{2Mr^3}{r^4 + a^2z^2}\left[\frac{r(xdx + ydy) - a(xdy - ydx)}{r^2 + a^2} + \frac{zdz}{r} + d\tilde{t}\right]^2. \end{aligned} \tag{2.16}$$

The surfaces of constant r are confocal ellipsoids in the $(x, y, z)-$plane, which degenerate for $r = 0$ to the disc $x^2 + y^2 \leq a^2, z = 0$. Fig. 2.1 shows the surface (2.15) projected on the plane $y = 0$ for different values of $r = 0$, 0.5 and 1. From Eqs. (2.12, 2.13) one can see that $\theta = \frac{\pi}{2}$, i.e. $z = 0$, corresponds to the boundary of the disc $x^2 + y^2 = a^2$ and so the curvature singularity, $\Sigma = 0$, can be interpreted as a *ring singularity*:

$$x^2 + y^2 = a^2,\ z = 0. \tag{2.17}$$

If $a^2 > M^2$, $r_\pm$ are complex, so Δ has no real zeros and the only existing singularities will be the ones from the previous analysis. But if $a^2 < M^2$, the metric still has the ring singularity but it is also singular at $r = r_\pm$, these being coordinate singularities. Defining new coordinates known as Kerr coordinates, v and χ, by

$$dv = dt + \frac{(r^2 + a^2)}{\Delta}dr, \tag{2.18}$$

$$d\chi = d\phi + \frac{a}{\Delta}dr, \tag{2.19}$$

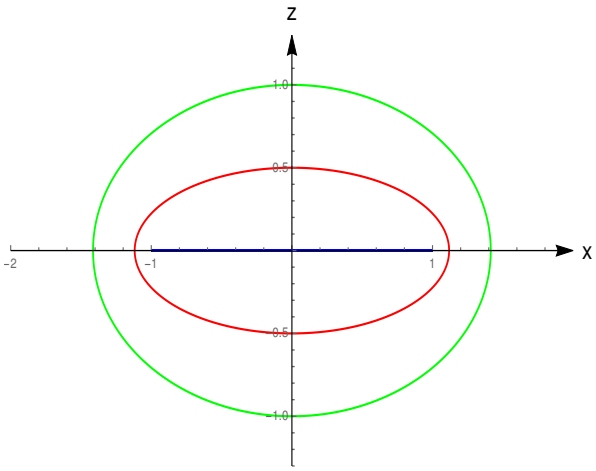

FIGURE 2.1: Contour plots of the surface $r(x, y = 0, z)/a$ for constant values 0 (blue), 0.5 (green) and 1 (red).

which are analogous to ingoing radial null coordiante for Schwarzschild, the metric takes the form

$$ds^2 = -\frac{\Delta - a^2 \sin^2\theta}{\Sigma} dv^2 + 2dvdr - \frac{2a\sin^2\theta(r^2 + a^2 - \Delta)}{\Sigma} dvd\chi - \\ - 2a\sin^2\theta d\chi dr + \frac{(r^2 + a^2)^2 - \Delta a^2 \sin^2\theta}{\Sigma} \sin^2\theta d\chi^2 + \Sigma d\theta^2 \tag{2.20}$$

and the metric is no longer singular at $\Delta = 0$ [16]. The surface $r = r_+$ is the event horizon for the Kerr black hole.

Considering a particle in the Kerr space-time, its action is given by

$$S = -m\int d\tau = -m\int \sqrt{-g_{\mu\nu}dx^\mu dx^\nu}, \tag{2.21}$$

for τ the proper time and m the particle mass. A symmetry of the particle action is associated with a Killing vector field ξ which leaves the action invariant, i.e. $\Delta S = 0$. This is done by the Lie derivative

$$\mathcal{L}_\xi g_{\mu\nu} = 0 \implies \nabla_\mu \xi_\nu + \nabla_\nu \xi_\mu = 0. \tag{2.22}$$

With such vector field, there is a conserved charge $Q = \xi^\mu p_\mu$, where $p_\mu = mu_\mu$ and u_μ is the four-velocity of the particle. Taking into account that $u^\alpha \nabla_\alpha u^\beta = 0$ as the geodesic equation, it follows that

$$u^\alpha \nabla_\alpha Q = mu^\alpha u^\mu \nabla_\alpha \xi_\mu = 0, \tag{2.23}$$

using Eq. (2.22) and so this charge is constant along geodesics. In Boyer-Linquist coordinates, the Killing vectors for Kerr are

$$k = \frac{\partial}{\partial t}, \quad m = \frac{\partial}{\partial \phi}, \tag{2.24}$$

which leads to two conserved charges energy per unit mass ϵ and angular momentum per unit mass l,

$$\epsilon = g_{\mu\nu} k^{\mu} \frac{dx^{\nu}}{d\lambda}, \tag{2.25}$$

$$l = g_{\mu\nu} m^{\mu} \frac{dx^{\nu}}{d\lambda}, \tag{2.26}$$

with λ denoting an affine parameter. For free pointlike particles, the geodesic equations in the equatorial plane, i.e. $\theta = \frac{\pi}{2}$, are the following:

$$\dot{t} = \Delta^{-1}\Big[\Big(r^2 + a^2 + \frac{2a^2M}{r}\Big)\epsilon - \frac{2aM}{r} l\Big], \tag{2.27}$$

$$\dot{\phi} = \Delta^{-1}\Big[\frac{2aM}{r}\epsilon + \Big(1 - \frac{2M}{r}\Big) l\Big], \tag{2.28}$$

where the dot corresponds to differention with respect to the affine parameter of the geodesic. Considering an observer falling into the BH with timelike four-velocity and zero angular momentum, from Eqs. (2.27, 2.28) with $l = 0$, the angular velocity measured from infinity is

$$\Omega = \frac{\dot{\phi}}{\dot{t}} = \frac{2Mar}{r^4 + r^2a^2 + 2a^2Mr}. \tag{2.29}$$

One can see that, in fact, at infinity $\Omega = 0$ is consistent with the definition of the zero angular momentum observers. But $\Omega \neq 0$ at any finite distance and at the horizon

$$\Omega_H = \frac{a}{2Mr_+}. \tag{2.30}$$

This phenomenon is known as *frame dragging* and the observers are forced to co-rotate with the geometry [3].

There is also another Killing vector, which is normal to the event horizon, making it a Killing Horizon, given by

$$\xi = k + \Omega_H m, \tag{2.31}$$

where the following equation is obeyed

$$\xi^{\mu}\partial_{\mu}(\phi - \Omega_H t) = 0. \tag{2.32}$$

This leads to $\phi = \Omega_H t +$ constant on orbits of ξ. Since null geodesics of the horizon follow orbits of ξ, one can say that the black hole is rotating with angular velocity Ω_H [16].

2.2.2 Ergoregion and the Penrose Process

Aside from the event horzion, the Kerr black hole possesses another infinite-redshift surface outside the horizon. This surface is defined by the roots of $g_{tt} = 0$ and is known as *ergosurface*. Infinite-redshift in the sense that any light ray emitted from the ergosurface is observed with an infinite redshift at $r \to \infty$ [3]. This can be seen from Eq. (2.11) when considering a static observer at infinity

$$ds^2 = -\frac{\Delta - a^2 \sin^2\theta}{\Sigma} dt^2. \tag{2.33}$$

If τ is the proper time, then $ds^2 = -d\tau^2$ and the observer at infinity measures an infinite redshift if $\Delta - a^2 \sin^2\theta = 0$. Thus, this leads to the ergosurface exterior to the event horizon being defined at

$$r_{ergo}(\theta) = M + \sqrt{M^2 - a^2\cos^2\theta}. \tag{2.34}$$

Since $0 < \theta < \pi$, this surface is defined by the limits at $r = 2M$ and $r = r_+$. The region between the event horizon and the ergosurface is the *ergoregion*. This region is shown in Fig. 2.2.

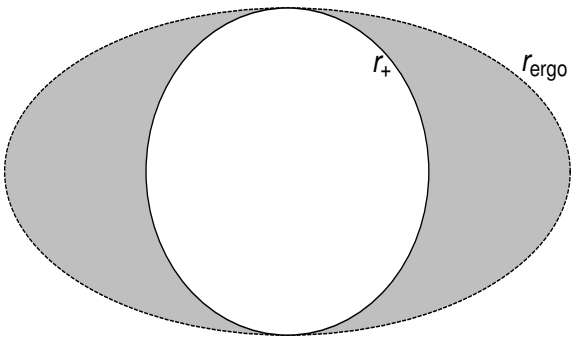

FIGURE 2.2: Ilustration of the ergoregion, grey zone bounded by the event horion r_+ and $r_{\text{ergo}}(\theta)$.

The ergoregion has the characteristic that the Killing vector field k becomes spacelike inside of this region, since

$$k^2 = k^\mu k^\nu g_{\mu\nu} = g_{tt}|_{ergoregion} > 0. \tag{2.35}$$

Considering a stationary observer at constant (r, θ), it has four-velocity $u^\mu = (\dot{t}, 0, 0, \dot{\phi})$. Due to causality, this observer needs to have a timelike orbit to exist, i.e. $u^2 < 0$. This leads to the following necessary condition for the existence of such an observer

$$g_{tt} + 2\Omega g_{t\phi} + \Omega^2 g_{\phi\phi} < 0. \tag{2.36}$$

The latter, Eq. (2.36), has as roots

$$\Omega_\pm = \frac{-g_{t\phi} \pm \sqrt{\Delta}\sin\theta}{g_{\phi\phi}} \tag{2.37}$$

and, thus, the existence of a stationary observer is not possible in the region $r_+ < r < r_-$ since $\Delta < 0$ [3]. On the outer horizon, $r = r_+$, one has that the only possible stationary observer has

$$\Omega_\pm = -\frac{g_{t\phi}}{g_{\phi\phi}} = \Omega_H, \tag{2.38}$$

which is the same as Eq. (2.30).

Considering a particle with mass m following a geodesic in the Kerr geometry, from Eq. (2.25) one see that the conserved charge is the energy $E = m\epsilon$ of the particle as measured from infinity. Supposing that the particle decays into two others with momenta q_1 and q_2, the particle q_1 falls into the black hole and the q_2 escapes the ergoregion. From the conservation of four-momentum and contracting with k, one has that

$$E = E_1 + E_2. \tag{2.39}$$

If this particle decays in the erogregion, one of the particles can have negative energy since k becomes spacelike in this region. Then, with $E_1 < 0$, one obtains that

$$E_2 = E + |E_1| > E, \tag{2.40}$$

and so the particle q_2 leaves the ergoregion with an energy greater than the energy of the original particle. The existence of an ergoregion thus allows one to extract energy from the

black hole [16]

As we have seen, an asymptotic observer may measure a particle energy as negative. But for a stationary observer at the horizon this particle must have $q_1 \cdot \xi \leq 0$, since $\xi^2 = 0$ and $q_1^2 \leq 0$. Using the expresson of Eq. (2.31) and $L_1 = -m \cdot q_1$, it results

$$E_1 - \Omega_H L_1 \geq 0. \tag{2.41}$$

The change in the BH mass is $\delta M = E_1$ and in the BH angular momentum is $\delta L = L_1$ so

$$\delta J \leq \frac{2M(M^2 + \sqrt{M^4 - J^2})}{J} \delta M, \tag{2.42}$$

which is analogous to

$$\delta(M^2 + \sqrt{M^4 - J^2}) \geq 0. \tag{2.43}$$

The previous equation is known as $\delta A \geq 0$, where A is the "area of the event horizon" of a Kerr black hole. Thus, energy extraction by Penrose process is limited by the condition $\delta A \geq 0$, i.e. the area of the event horizon must increase [16, 17].

2.3 Superradiant Scattering

Superradiant scattering involves the process of radiation amplification. This process can be traced back to the dawn of quantum mechanics when studying the scattering of fermions, and later, the scattering of bosons [21, 22].

2.3.1 Bosonic Scattering

Considering a massive scalar field Φ minimally coupled to an eletromagnetic potential $A_\mu = (\phi, 0)$, where for simplicity one just considers one spatial dimension, its dynamics is described by the Klein-Gordon equation

$$\left(\nabla^\mu \nabla_\mu - \mu^2\right)\Phi = 0. \tag{2.44}$$

The derivative is defined as $\nabla_\mu = \partial_\mu + ieA_\mu$ and e is the charge of the field.

Choosing the *ansatz* $\Phi = e^{-i\omega t}u$, the equation to be solved is

$$\frac{d^2u}{dx^2} + [(\omega - e\phi)^2 - \mu^2]u = 0. \tag{2.45}$$

Taking the scenario $e\phi = V\Theta(x)$, Θ being the Heaviside step function, and a beam of particles coming from $-\infty$ which scatters off the potential, the solutions of (2.45) are

$$u_I = \mathcal{A}e^{ikx} + \mathcal{B}e^{-ikx}, \quad x < 0, \tag{2.46}$$

$$u_{II} = \mathcal{C}e^{ipx}, \quad x > 0, \tag{2.47}$$

where $k = \sqrt{\omega^2 - \mu^2}$ and $p = \pm\sqrt{(\omega - e\phi)^2 - \mu^2}$. The sign of the momentum p must be chosen carefully. If particles are transmitted by the potential barrier, they must go to $+\infty$ and so their velocity must be positive [3, 21]. Computing the group velocity, one has

$$\frac{\partial\omega}{\partial p} = \frac{p}{\omega - e\phi} > 0. \tag{2.48}$$

Normalizing $\mathcal{C}$ to unity, one can calculate the coefficents $\mathcal{A}$ and $\mathcal{B}$ through continuity at $x = 0$, which gives the transmission and reflection coefficents as

$$R = \frac{|\mathcal{B}|^2}{|\mathcal{A}|^2} = \frac{(1-\beta)^2}{(1+\beta)^2}, \quad T = \frac{k|\mathcal{C}|^2}{p|\mathcal{A}|^2} = \frac{4\beta}{(1+\beta)^2}. \tag{2.49}$$

with $\beta = \frac{p}{k}$ [21]. In the strong potential regime $\omega - e\phi + \mu < 0$ leads to $\text{sign}(p) < 0$ and $\beta < 0$. This implies that the wave is amplified when reflected by the potential since $R > 1$.

2.3.2 Fermionic Scattering

Now considering the Dirac equation for a 1/2-spin massive fermion Ψ, coupled to the same eletromagnetic potential A_μ as before, one has

$$(i\gamma^\mu \nabla_\mu - \mu)\Psi = 0, \tag{2.50}$$

where γ^μ are the Dirac gamma matrices. The solutions can be written as $\Psi = e^{-i\omega t}\psi$ and the equation to be solved is

$$i\gamma^x \partial_x \psi + [\gamma^0(\omega - e\phi) - \mu]\psi = 0. \tag{2.51}$$

In a choosen representation, the gamma matrices are

$$\gamma^0 = \begin{bmatrix} 1 & 0 \\ 0 & -1 \end{bmatrix}, \quad \gamma^x = \begin{bmatrix} 0 & 1 \\ -1 & 0 \end{bmatrix},$$

and the solutions are

$$\psi_I = \mathcal{A}\begin{bmatrix} 1 \\ \frac{k}{\omega+\mu} \end{bmatrix} e^{ikx} + \mathcal{B}\begin{bmatrix} 1 \\ \frac{-k}{\omega+\mu} \end{bmatrix} e^{-ikx}, \quad \psi_{II} = \mathcal{C}\begin{bmatrix} 1 \\ \frac{p}{\omega-e\phi+\mu} \end{bmatrix} e^{ipx}.$$

Using the same procedure as before, one obtains the reflection and transmission coefficents

$$R = \left[\frac{1-\beta}{1+\beta}\right]^2, \quad T = \frac{4\beta}{(1+\beta)^2}, \tag{2.52}$$

with $\beta = \frac{p}{k}\frac{\omega+\mu}{\omega-e\phi+\mu}$ [21]. In the strong potential regime, $\omega - e\phi + \mu < 0$, leads to $\text{sign}(p) < 0$ but since now $\beta > 0$, the reflection coefficent is $R < 1$ and there is no amplication of the wave.

2.4 Black Hole Superradiant Instabilities

Since the Kerr metric is stationary, a field in such a spacetime will vary in time as

$$\Psi \propto e^{-i\omega t}. \tag{2.53}$$

Unstable particles have a complex frequency $\omega - i\Gamma$, where Γ is the decay width of the particle. Analogously, if $\omega = \omega_R + i\omega_I$, one has that the number of particles goes as

$$|\Psi|^2 \propto e^{2\omega_I t}. \tag{2.54}$$

Thus, if $\omega_I > 0$, the number of particles will grow in time. As we will see in the following sections, the particles will form bound states with the black hole and the condition for the imaginary part of the bound state frequency to be positive, i.e. to grow exponentially, is

$$\omega_R < m\Omega_H, \tag{2.55}$$

where m is the quantum azimuthal number along the axis of rotation and Ω_H is the angular velocity of the black hole already found in previous sections.

2.4.1 General Formalism

In this work, we will study superradiant instabilities of a massive scalar field in a Kerr spacetime background. To do so, one uses the metric of Eq. (2.11) and

$$\left(g^{\mu\nu}\nabla_\mu\nabla_\nu - \mu^2\right)\Psi = \frac{1}{\sqrt{-g}}\partial_\mu\left(\sqrt{-g}g^{\mu\nu}\partial_\nu\Psi\right) - \mu^2\Psi = 0, \tag{2.56}$$

where μ is the mass of the field and g is the determinant of the metric, which results in $\sqrt{-g} = \Sigma \sin\theta$. Since the metric is independent of t and ϕ, one makes the *ansatz*

$$\Psi = e^{im\phi - i\omega t} S(\theta) R(r), \tag{2.57}$$

for some functions $S(\theta)$ and $R(r)$ [23]. Considering this *ansatz*, Eq. (2.56) is separable into two other differential equations, $\hat{L}_\theta \Psi = -\lambda \Psi$ and $\hat{L}_r \Psi = \lambda \Psi$, in which $\hat{L}_\theta \Psi + \hat{L}_r \Psi = 0$:

$$\frac{1}{\sin\theta}\partial_\theta\Big(\sin\theta \partial_\theta S\Big) + \Big[a^2(\omega^2 - \mu^2)\cos^2\theta - \frac{m^2}{\sin^2\theta} + \lambda\Big] S = 0, \tag{2.58}$$

$$\Delta \partial_r\Big(\Delta \partial_r R\Big) - \Delta\Big[\mu^2 r^2 + a^2\omega^2 - 2\omega m a r + \lambda + (\omega(r^2 + a^2) - ma)^2\Big] R = 0. \tag{2.59}$$

The separation constant correspondes to the eigenvalue of the angular spheroidal harmonic Eq. (2.58) and is given by

$$\lambda = l(l+1) + \sum_{k=1}^{\infty} C_{klm}(aq)^{2k}, \tag{2.60}$$

where $q = \sqrt{\mu^2 - \omega^2}$ and the coefficients C_{jlm} can be found in [24].

It is possible to rewrite Eq. (2.59), choosing as new variable $x = (r - r_+)/r_+$ and using $\tau = (r_+ - r_-)/r_+$, as

$$x^2(x+\tau)^2 \partial_x^2 R + x(x+\tau)(2x+\tau)\partial_x R + V(x) R = 0, \tag{2.61}$$

$$V(x) = [(x+\tau)x\overline{\omega} + (2-\tau)(\overline{\omega} - m\overline{\Omega}_H)]^2 + \\ + x(x+\tau)[(\tau-1)\overline{\omega}^2 + 2(2-\tau)\overline{\omega} m \overline{\Omega}_H - \overline{\mu}^2(x+1)^2 - \lambda]. \tag{2.62}$$

The barred quantities are defined as $\overline{\beta} = r_+ \beta$ and are dimensionless [23].

2.4.2 Results

The radial equation (2.59) does not have an exact analytical solution but for small masses $\overline{\mu} \ll 1$ one can divide the exterior of the black hole into two overlapping regions - a near-horizon region, $\overline{\omega} x \ll l$, and a far-region, $x >> 1$, where the function R has an analytical solution in both regions, and match both solutions in the region $1 \ll x \ll \frac{l}{\overline{\omega}}$ [25].

In the near-horizon region, one has:

$$x^2(x+\tau)^2 \partial_x^2 R + x(x+\tau)(2x+\tau)\partial R + V(x) R = 0, \tag{2.63}$$

$$V(x) \approx \Big[(2-\tau)(\overline{\omega} - m\overline{\Omega}_H)\Big]^2 - \lambda x(x+\tau) \tag{2.64}$$

where one defines $\overline{\omega} = (2-\tau)(\overline{\omega} - m\overline{\Omega}_H)$.

One has to impose ingoing boundary conditions at the event horizon since no waves can escape the BH, giving:

$$R(r \to r_*) \sim e^{-i(\omega - m\Omega_H)r_*}. \tag{2.65}$$

Using $r_* \equiv r_*(r)$ and x to write $r_* \equiv r_*(x)$, one arrives at

$$R(x \to 0) \sim \left(\frac{x}{x+\tau}\right)^{-\frac{i\overline{\omega}}{\tau}}. \tag{2.66}$$

Due to the boundary condition (2.66) and to assure continuity, one chooses the *ansatz* $R_{near}(x) = A\left(\frac{x}{x+\tau}\right)^{-\frac{i\overline{\omega}}{\tau}} f(x)$. From Eq. (2.63), f is a solution of the hypergeometric differential equation [24] and the near-horizon solution is

$$R_{near}(x) = A\left(\frac{x}{x+\tau}\right)^{-\frac{i\overline{\omega}}{\tau}} {}_2F_1\left(l+1, -l, 1 - \frac{i2\overline{\omega}}{\tau}, -\frac{x}{\tau}\right). \tag{2.67}$$

Using the asymptotic properties of the hypergeometric function [24], taking the limit $x \gg \tau$ of Eq. (2.67), one obtains

$$R_{near}(x) \approx A\Gamma\left(1 - \frac{2i\overline{\omega}}{\tau}\right)\left[\frac{\Gamma(-2l-1)}{\Gamma(-l)\Gamma(-l-2i\overline{\omega}/\tau)}\left(\frac{x}{\tau}\right)^{-l-1} + \right.$$
$$\left. + \frac{\Gamma(2l+1)}{\Gamma(l+1)\Gamma(l+1-2i\overline{\omega}/\tau)}\left(\frac{x}{\tau}\right)^{l}\right]. \tag{2.68}$$

In the far region, one has:

$$x^2\partial_x^2 R + 2x\partial_x R + (-\overline{q}^2x^2 + 2\overline{q}\nu x - \lambda)R = 0, \tag{2.69}$$

where

$$\nu = \left(\frac{2-\tau}{2}\right)\left(\frac{\overline{\omega}^2 - \overline{q}^2}{\overline{q}}\right). \tag{2.70}$$

Eq. (2.69) takes a similar form as the hydrogen-atom equation and its solution is given in terms of a confluent hypergeometric function [24]

$$R_{far}(x) = Bx^l e^{-\bar{q}x} U(l+1-\nu, 2l+2, 2\bar{q}x). \tag{2.71}$$

Taking the limit $\bar{q}x \ll 1$, it reduces to [24]

$$R_{far}(x) \approx B\frac{\pi}{\sin((2l+2)\pi)}\Big[\frac{x^l}{\Gamma(-l-\nu)\Gamma(2l+2)} - \frac{2\bar{q}^{-(2l+1)}}{\Gamma(l+1-\nu)\Gamma(-2l)}x^{-l-1}\Big]. \tag{2.72}$$

One can see that the solutions present the same behaviour in their common domain of validity. To obtain the spectrum of the quase-bound states, one matches the coefficients of x^l and x^{-l-1}, which gives the condition:

$$\frac{\Gamma(-l-\nu)\Gamma(2l+2)]}{\Gamma(l+1-\nu)\Gamma(-2l)} = -(2\bar{q}\tau)^{2l+1}\frac{\Gamma(-2l-1)\Gamma(l+1)\Gamma(l+1-2i\overline{\omega}/\tau)}{\Gamma(-l)\Gamma(2l+1)\Gamma(-l-2i\overline{\omega}/\tau)}. \tag{2.73}$$

Since for bound states $\bar{q} \ll 1$ in the small mass limit $\mu M \ll 1$, one has that to leading order,

$$\frac{\Gamma(-l-\nu)\Gamma(2l+2)]}{\Gamma(l+1-\nu)\Gamma(-2l)} = 0 \implies l+1-\nu^{(0)} = -n_r, \tag{2.74}$$

from the properties of the gamma function [24] where n_r is a non-negative integer. From Eq. (2.70), its possible to solve for the bound state frequency, $\overline{\omega} = \overline{\omega}^{(0)} + \delta\overline{\omega}$, where $\overline{\omega}^{(0)} = \overline{\mu}$. This yields a Hydrogen-like spectrum in a gravitational field:

$$\delta\overline{\omega} = -\Big(\frac{2-\tau}{2}\Big)^2\frac{\overline{\mu}^3}{2(l+1+n_r)^2} = -\overline{\mu}\frac{(\mu M)^2}{2(l+1+n_r)^2} \equiv -\overline{\mu}\frac{(\mu M)^2}{2n^2}, \tag{2.75}$$

where $n = l+1+n_r$. This result is not surprising since particles are bound by the BHs $1/r$ gravitational potential to leading order. To evaluate if the mode is stable or unstable, one needs to compute the imaginary part of the bound state frequency ω_I. To do this [23, 26], one can expand the lefthand side of Eq. (2.73) with $\nu = \nu^{(0)} + \delta\nu$ and evaluate the righthand side with the leading order result $\omega^{(0)}$. To cancel the poles in the gamma functions, one uses the the following results (See Appendix B):

$$\lim_{z\to -n}\frac{\psi(z)}{\Gamma(z)} = (-1)^{n+1}n!, \quad \frac{\Gamma(-2l-1)}{\Gamma(-l)} = \frac{(-1)^{l+1}}{2}\frac{l!}{(2l+1)!},$$
$$\frac{\Gamma(l+1-y)}{\Gamma(-l-y)} = (-1)^l x\prod_{k=1}^{l}(k^2-y^2). \tag{2.76}$$

One defines $F(\nu)$ as

$$F(\nu) \equiv \frac{\Gamma(-l-\nu)}{\Gamma(l+1-\nu)} \approx F(\nu^{(0)}) + F'(\nu)|_{\nu^{(0)}}\delta\nu + \mathcal{O}(\delta\nu^2), \tag{2.77}$$

$$F'(\nu) = F(\nu)[\psi(-l-\nu) - \psi(l+1-\nu)]. \tag{2.78}$$

Since $F(\nu^{(0)}) \to 0$, and using the first result from (2.76), it results

$$\begin{aligned} F(\nu) &\approx -\Gamma(-l-\nu^{(0)}) \lim_{\nu\to\nu^{(0)}} \frac{\psi(l+1-\nu)}{\Gamma(l+1-\nu)} \\ &= -\Gamma(-2l-1-n_r)(-1)^{n+1}n_r!. \end{aligned} \tag{2.79}$$

The left-hand side (LHS) of Eq. (2.73) becomes

$$\text{LHS} \cong -\frac{(2l+1)!n_r!(2l)!}{(2l+1+n_r)!}\delta\nu. \tag{2.80}$$

From the definition of q which appears in (2.60) and the spectrum (2.75), one can expand q with $\omega = \omega^{(0)} + \delta\omega$ to obtain

$$\bar{q} \approx \frac{r_+ M\mu^2}{(l+1+n_r)}, \tag{2.81}$$

and using the second and third results from (2.76) with $y = 2i\overline{\omega}/\tau$, the right-hand side (RHS) of Eq. (2.73) becomes

$$\text{RHS} \cong \left(\frac{2r_+M\mu^2\tau}{l+1+n_r}\right)^{2l+1}\frac{1}{2}\frac{l!}{(2l+1)!}\frac{l!}{(2l)!}\left(\frac{2i\overline{\omega}}{\tau}\right)\prod_{k=1}^{l}\left(k^2 - \left(\frac{2i\overline{\omega}}{\tau}\right)^2\right). \tag{2.82}$$

Matching LHS = RHS, one obtains $\delta\nu$ which is related with $\delta\omega$ by $\delta\omega = \frac{\partial\omega}{\partial\nu}\delta\nu$. Noticing that

$$2r_+\tau = (4M)^{2l+1}\left(\frac{r_+ - r_-}{r_+ + r_-}\right)^{2l+1}, \tag{2.83}$$

one finally obtains the imaginary part of the bound state frequency, ω_I,

$$\omega_I M = -\frac{1}{2}A_{ln_r}(\varpi M)(\mu M)^{4l+5}\left(\frac{r_+ - r_-}{r_+ + r_-}\right)^{2l+1}, \tag{2.84}$$

with

$$A_{ln_r} = \left[\frac{l!}{(2l+1)!(2l)!}\right]^2\frac{(2l+1+n_r)!}{n_r!}\frac{4^{2l+1}}{(l+1+n_r)^{2l+4}}\prod_{j=1}^{l}\left(j^2 + 16\left(\frac{\varpi M}{\tau}\right)^2\right). \tag{2.85}$$

For an unstable mode, the imaginary part needs to be positive, $\omega_I > 0$, and this leads to

$$\varpi < 0 \implies \omega_R < m\Omega_H, \tag{2.86}$$

which is known as the *superradiant condition*. It can be written in a more natural form, in the small mass limit and $\tilde{a} = 1$ [27], as

$$\alpha_\mu \equiv \frac{\mu M G}{\hbar c} < \frac{1}{2}. \tag{2.87}$$

The dimensionless constant α_μ is the gravitational analogous of the fine structure constant since it appears in Eq. (2.75) when one converts to SI units, i.e. $\mu M \to \alpha_\mu$.

The analytical expression of the imaginary part of the frequency is only valid for small α_μ. Numerical methods are thus required to compute the full spectrum for general masses and BH spins. The numerical method used here is the same as [23] and other analyses can be found in [26, 28].

Near the horizon, the radial function takes the form of Eq. (2.67), and for $x \ll 1$ one can Taylor expand it:

$$R_{near}(x) = x^{-i\frac{\varpi}{\tau}} \sum_{n=0}^{\infty} a_n x^n \,. \tag{2.88}$$

The coefficents a_n can be calculated by substituiting this *ansatz* into Eq. (2.61) and using Mathematica to solve it order by order. One can set $a_0 = 1$ since normalization is not relevant in computing the spectrum. After obtaining the desired series, one can solve the differential equation (2.61) taking as boundary conditions for $x = \epsilon \ll 1$ the solution (2.88) and integrating it out to a sufficiently large distance from the horizon, $x = d$, as a function of the frequency ω. Thus, bound states will correspond to states for each (l, m) that minimize $R(d)$ in the complex $\omega-$plane and this can all be done with Mathematica.

In Fig. 2.3 we show the analytical and numerical results for the imaginary part of the bound state frequency for the fastest mode [28], $l = m = 1$ and $n = 2$, and for different values of the black hole spin $\tilde{a}$.

Since we are interested in working with some analytical results, we tried to adjust the function (2.84) to the numerical results. The first step to do is to define the "adjusted" function

$$(\omega_I M)_{adjusted} = (\omega_I M)_{analytical} \times (1 + f), \tag{2.89}$$

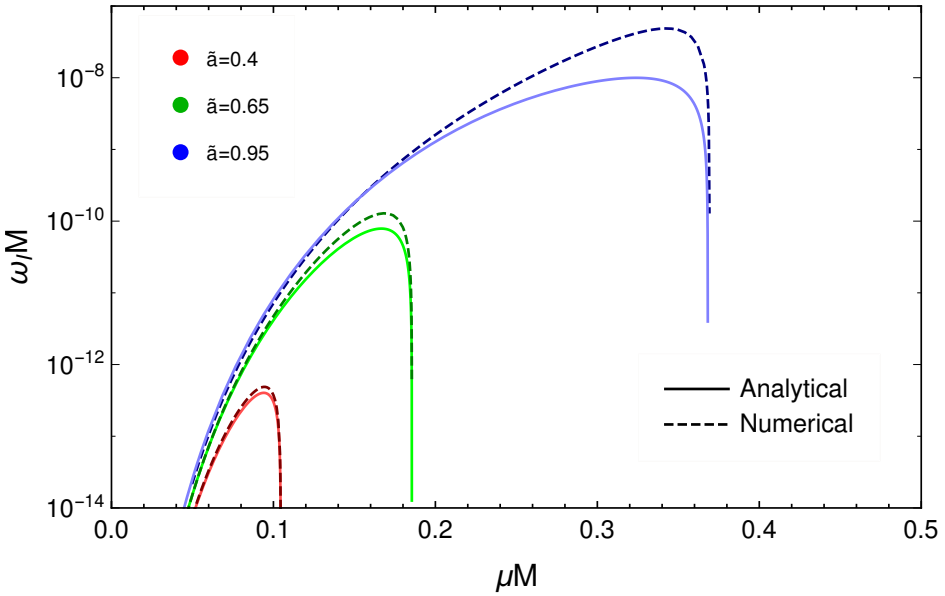

FIGURE 2.3: Imaginary part of the bound state frequency for the fastest mode as a function of the dimensionless coupling μM.

where f will be a function of the spin and mass of the black hole, $\tilde{a}$ and α_μ, i.e. $f \equiv f(\alpha_\mu, \tilde{a})$, and $(\omega_I M)_{analytical}$ is given by Eq. (2.84) with the values of l, m and n for the fastest mode. We know that the function $(\omega_I M)_{analytical}$ works well for small values of mass and spin, so an *ansatz* for the function f is

$$f = \sum_{n\geq 2} \left(c(\tilde{a}) \left(\frac{\alpha_\mu}{\Omega_H M} \right)^n \right), \tag{2.90}$$

where $\Omega_H M = \frac{\tilde{a}}{2(1+\sqrt{1+\tilde{a}^2})}$, and $n \geq 2$ such that f is of order $\mathcal{O}(\alpha_\mu^2)$ or greater for small mass. We found that the form of function f which fits better with the numerical results is

$$f = c(\tilde{a}) \left(\frac{\alpha_\mu}{\Omega_H M} \right)^6, \tag{2.91}$$

where we used Mathematica to obtain $c(\tilde{a})$. The coefficent $c(\tilde{a})$ is computed by evaluating f for various values of spin $\tilde{a}$ and making a fit for the different values of the coefficent. This is shown in Fig. 2.4.

The final form of the function f is

$$f = 1.5 \frac{\tilde{a}^{9/5}}{\sqrt{1-\tilde{a}}} \left(\frac{\alpha_\mu}{\Omega_H M} \right)^6, \tag{2.92}$$

and the imaginary part (2.89) takes the form

$$(\omega_I M)_{ajusted} = -\frac{1}{2} A_{1,0} \left(\frac{\varpi M}{\tau} \right) (\mu M)^9 \left(\frac{r_+ - r_-}{r_+ + r_-} \right)^3 \left(1 + 1.5 \frac{\tilde{a}^{9/5}}{\sqrt{1-\tilde{a}}} \left(\frac{\alpha_\mu}{\Omega_H M} \right)^6 \right). \tag{2.93}$$

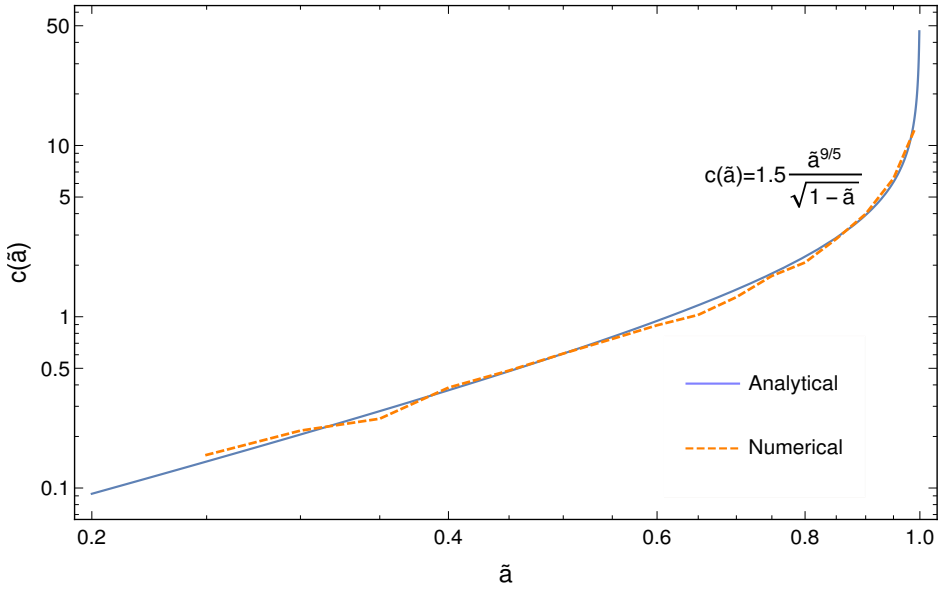

FIGURE 2.4: Coefficient $c(\tilde{a})$ as a function of $\tilde{a}$ and the obtained fit.

Fig. 2.5 shows the numerical results and the ajusted function for the imaginary part.

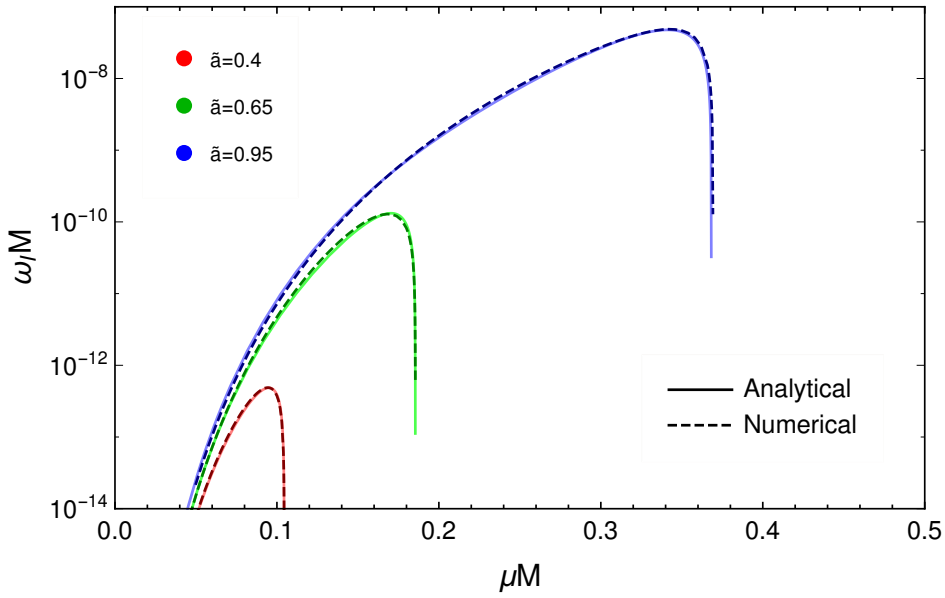

FIGURE 2.5: Imaginary part of the bound state frequency for the fastest superradiant mode with the added corrections as a function of the dimensionless coupling μM.

Since all of the latter is done by numerical methods, there is an associated error which is propagated through all the process. Our purpose in this section is not to have an exact treatment of the results but to have an analytical object that we can work with in our subsequent analysis. This being said, our tolerance for the difference between the function $(\omega_I M)_{adjusted}$ and the numerical results is an error up to $\sim 50\%$, i.e. the order of magnitude to be correct. The average error associated to various values of $\tilde{a}$ is shown in Fig. 2.6.

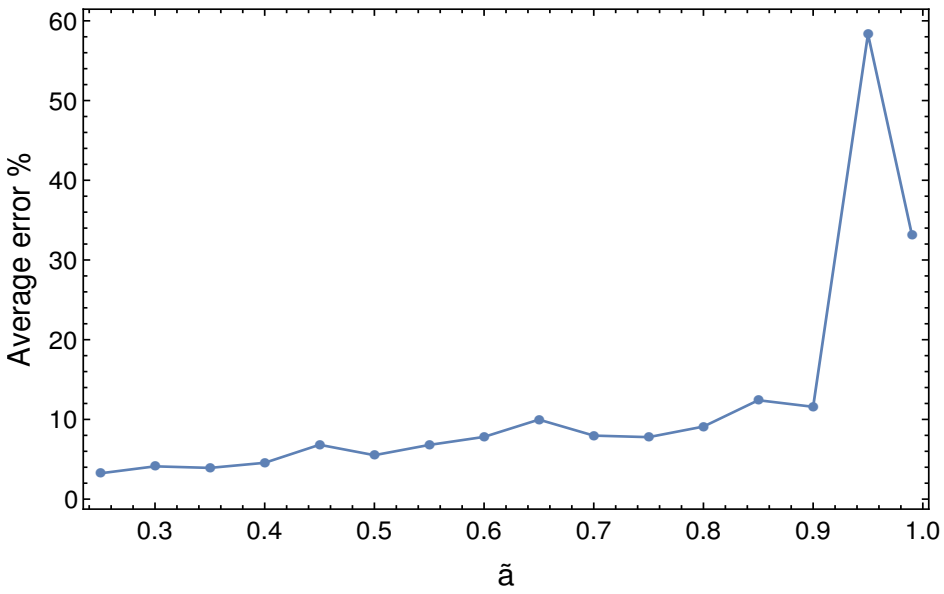

FIGURE 2.6: Average relative errors between the $(M\omega)_{\text{analytical}}$ and $(M\omega)_{\text{adjusted}}$ for several values of $\tilde{a}$.

2.5 Superradiance and Particle Physics

Black holes are known to be a great theoretical laboratory to probe high energy physics, mainly when one conjugates the phenomenon of superradiance with particle physics [8, 9], not only because they provide tools to do so but also since there is a significant interest in black hole observations in astronomy. From previous sections, one saw that when a massive bosonic field is present in a Kerr spacetime, it can affect the dynamics of a black hole by extracting mass and spin from it. The superradiant condition tells us what kind of black holes with mass M can produce superradiant instabilities in a bosonic field with mass μ. Most astrophysical black holes, such as black holes in the center of galaxies, have very large masses which implies that the particles described by the bosonic field must be very light. The most notable candidate to be studied in a such environment is the QCD axion. The axion was first postulated to solve the strong CP problem in QCD [10] and later arising in the context of string theory, more concretely in the string vacua which leads to the expectation of a number of axion-like fields known as *axiverse* [29, 30]. Some processes that could lead to the observation of the axion effects is the fact that when under superradiant instabilities, the non-linear effects in the transitioning of "atomic" levels in a cloud around the black hole could generate gravitational waves and the annihilation of axions into gravitons [31]. Another process known as *black hole bombs* consists in the stimulation of the axion decay into photons [27]. This would lead to extreme high cloud luminosities in the vicinity of a black hole suggesting a possible link to the observed fast radio bursts. Besides the axion, there are also a great interest in studying vector and tensor fields under superradiant instabilities since these are also predicted in several Beyond the Standard Model scenarios [32, 33]. If one considers heavy instead of light bosonic fields, the black holes that could produce superradiant instabilities would need to be very light. Due to their lightness, these black holes need to be formed in the early universe. Thus, studying the superradiant effects of heavy particles on the dynamics of black holes can yield information not only about the black holes themselves but also about early universe cosmology.

Chapter 3

Pions

There was a time in particle physics when one of the main questions was the stability of the nucleus. Since the proton has a charge and this is confined on such a small space, the eletromagnetic force should repel the existing protons in the nucleus making them separate from each other. But since this was not happening, there should another force, stronger than the eletromagnetic force, that was keeping the nucleus together, known as the $strong force$. The first significant theory of the strong force was proposed by Hideki Yukawa in 1934 [34] which stated that the carrier of the nuclear force sould be a particle, i.e. the proton and the neutron should be attracted by a field, just like the eletromagnetic field or the gravitational field. This particle would be known as the *pion*. In 1947 it was discovered that there were two particles in cosmic rays, one corresponding to the Yukawa predicted particle and the other would be known as the *muon* [35].

3.1 Quantum Chromodynamics (QCD)

3.1.1 Quark Model

In the first years of studying the nuclear force (strong interaction), it was found that, to a good approximation, this is independent of the electric charge carried by the nucleons. Since the proton and the neutron have almost the same mass, Heisenberg introcuced the *isospin* symmetry in which the proton $|p\rangle$ and the neutron $|n\rangle$ are considered two states of a single particle. Being more specific, the strong interaction is invariant under an isospin transformation [19].

The current theoretical picture of the strong interactions began when one realized that the elementary particles that make up the proton and other *hadrons* are fermions called *quarks* (q). The lightest *mesons* and *baryons* can be described by three elementary quarks, up (u),

down (d) and strange (s), although one knowns that actually there are six *flavours* of quarks. Within the same mind set as Heisenberg, the similarity between some mesons and baryons masses suggests the existence of a symmetry between the quark constituents. This idea was followed after the construction of the *Eightfold Way* [36]. The principle is that each hadron is composed by quarks and that these quarks are related by SU(3) transformations, in which the fundamental representation **3** is $(u, d, s)^T$ [1]. Their antiparticles, called *antiquarks*, are in the conjugate complex representation $\overline{\mathbf{3}}$ with a basis $(\overline{u}, \overline{d}, \overline{s})^T$, where they have quantum numbers opposite to the corresponding particle, i.e. being N the quantum number, then $N_{\overline{q}} = -N_q$. The quarks and antiquarks can be put on a diagram of *Isospin* T_3 vs *Hypercharge* $Y = \frac{2}{\sqrt{3}} T_8$ where T_3 and T_8 are the diagonals generators of SU(3) [1]. This is shown in Fig. 3.1.

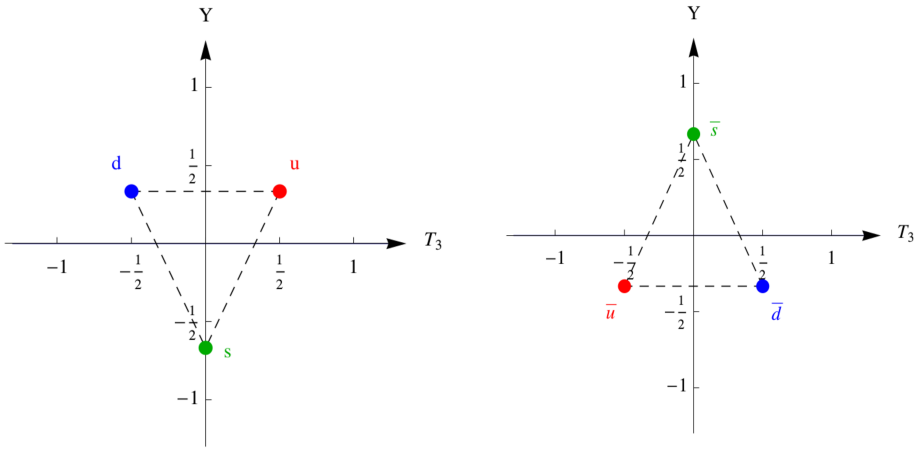

FIGURE 3.1: Isospin vs Hypercharge diagrams. In the left diagram are decipted the quarks and in the right diagram are decipted the anti-quarks [1].

One can also define the charge of the quarks as

$$Q = T_3 + \frac{Y}{2}. \tag{3.1}$$

Thus, hadrons are now composite states of these elementary particles. The mesons are spin-0 bound states of a quark and an anti-quark. In the context of SU(3), the mesons must lie in the tensor product representation,

$$\mathbf{3} \times \overline{\mathbf{3}} = \mathbf{8} + \mathbf{1}. \tag{3.2}$$

The baryons are a bound state of three quarks and must lie in the tensor product representation,

$$\mathbf{3} \times \mathbf{3} \times \mathbf{3} = \mathbf{10} + \mathbf{8} + \mathbf{8} + \mathbf{1}. \tag{3.3}$$

Focusing on the baryons, inside the octet, if one keeps s fixed and interchange the other quarks, one obtains a symmetry analogous to the symmetry postulated by Heisenberg between the neutron and the proton. In this context, the symmetry is also known as isospin. We will be interested in the states that have null hypercharge, corresponding to an isospin triplet of value one. These composite states are the pions:

$$\pi = \begin{bmatrix} \pi^+ & \pi^0 & \pi^- \end{bmatrix}.$$

The quark model lies in the approximation that the masses of the quarks are similiar but this can only be done in certain conditions, as one will see. The fact that the quark model still applies, in the sense that the flavour symmetry is a good approximation, is that the binding energy of the mesons and baryons are of the order of 1 GeV, where differences between the masses of the strange and up/down are of the order of 100 MeV [37]. It is curious to notice that the isospin symmetry is more robust than the flavour symmetry, since the relations between the quarks masses are $m_u \approx m_d$ and $m_s \gg m_{u,d}$.

Despite the sucess in formulating and cataloguing the diverse zoo of hadrons, this models has two main problems. One is due to the fact that no one has ever seen an individual quark. This might seem strange since quarks should be "easy" to recognize because of the feature of carrying fractional charge. This led physicists to postulate that quarks should be confined inside the hadrons, i.e. they are always attached to other quarks. This postulate is known as *quark confinement*. The other problem is that some hadrons, namely baryons, can be composed by only one type of quark, such as the case of $\Delta^{++} \sim uuu$. Since quarks are fermions, they need to respect the Pauli Principle and so in 1964 it was postulated that quarks should carry another quantum number known as *color charge*. This model assigns quarks to the fundamental representation of a new internal SU(3) symmetry, i.e. $q \to (q_R, q_B, q_G)^T$ transforms under SU(3). With the color charge in the quark model, the confinement postulate becomes that the wavefunction of hadrons needs to be "white", i.e. the wavefunction needs to be a color singlet [35, 37].

3.1.2 QCD Lagrangian

When introducing the color symmetry $SU(3)_c$, a quark becomes a color triplet $q = (q_R, q_G, q_B)^T$. For the sake of simplicity, one considers only a single flavour, then it can be generalized by considering $q = q_i$ where i is a flavour index. Under an $SU(3)_c$ transformation

$$q \to q' = e^{i\alpha^a T_a} q, \tag{3.4}$$

where α is spacetime dependent and T_a are de generators of $SU(3)_c$. The free quark Lagrangian,

$$\mathcal{L}_D = \bar{q}(i\gamma^\mu \partial_\mu - m)q, \tag{3.5}$$

is not invariant under such tranformation. To solve this problem, one introduces a vector gauge field $A_\mu = A^a_\mu T_a$ to form the covariant derivative

$$D_\mu = \left(\partial_\mu - igA^a_\mu T_a\right). \tag{3.6}$$

One also introduces the field strength $F_{\mu\nu} = F^a_{\mu\nu} T_a$ associated with the vector gauge field A_μ

$$F^a_{\mu\nu} = \partial_\mu A^a_\nu - \partial_\nu A^a_\mu - ig[A_\mu, A_\nu]^a, \tag{3.7}$$

and the complete invariant Lagrangian [19, 20] reads

$$\mathcal{L}_{QCD} = -\frac{1}{4}\left(F^a_{\mu\nu}\right)^2 + \bar{q} i\gamma^\mu D_\mu q - m\bar{q}q. \tag{3.8}$$

Due to the invariance of Eq. (3.8), the gauge field and the field strength transform [19, 20] infinitesimally as,

$$A^a_\mu \to A^a_\mu + f^{abc}\alpha^b A^c_\mu - \frac{1}{g}\partial_\mu \alpha^a, \tag{3.9}$$

$$F^a_{\mu\nu} \to F^a_{\mu\nu} + f^{abc}\alpha^b F^c_{\mu\nu}. \tag{3.10}$$

If one expands the pure Yang-Mills term, $-\frac{1}{4}\left(F^a_{\mu\nu}\right)^2$, it can be seen that there are trilinear and quadrilinear terms in A^a_μ,

$$-gf^{abc}\partial_\mu A^a_\nu A^{b\mu} A^{c\nu} - \frac{g^2}{4} f^{abc} f^{ade} A^b_\mu A^c_\nu A^{d\mu} A^{e\nu}, \tag{3.11}$$

which correspond to self interations of non-Abelian gauge fields. From the second term of Eq. (3.9), one see that the gauge field transform in the adjoint representation of $SU(3)_c$ and so it carries charge. The gauge field is known as *gluon* and there are eight different gluons, as many as the number of generators of $SU(3)_c$. These gluons are massless and they are the mediators of the strong force between the quarks.

An important characteristic of QCD that distinguish it from other theories, such as QED and $\lambda\phi^4$ is that this theory presents asymptotic freedom. As the energy gets higher, the coupling constant becomes smaller making the interations of the gauge field and quarks weaker [20].

3.1.3 Effective field theory of QCD

As one mentioned, at high energy the theory of QCD presents asymptotic freedom and so it can be treated through perturbative methods. But, at low energies, this ceases to be true. However, for the lightest hadrons, namely the pion, their interactions can be treated using an effective field theory [19, 38].

Remembering the Lagrangian (3.8) considering only the quark flavours u and d, one reads

$$\mathcal{L} = \left(\overline{u} i\gamma^\mu D_\mu u - m_u \overline{u} u + \overline{d} i\gamma^\mu D_\mu d - m_d \overline{d} d\right) - \frac{1}{4}\left(F^a_{\mu\nu}\right)^2. \tag{3.12}$$

Considering only the kinectic part, ignoring the quark masses, if one uses the projector $(1 \pm \gamma_5)/2$ to separate right-handed and left-handed quarks respectively, the latter can be written as

$$\overline{u}_R i\gamma^\mu D_\mu u_R + \overline{u}_L i\gamma^\mu D_\mu u_L + \overline{d}_R i\gamma^\mu D_\mu d_R + \overline{d}_L i\gamma^\mu D_\mu d_L. \tag{3.13}$$

There is an embedded $SU(2)_L \times SU(2)_R$ symmetry, under which for if $q = (u,d)^T$, then $q_L \to Lq_L$ and $q_R \to Rq_R$, where L and R are independent matrices belonging to $SU(2)_L$ and $SU(2)_R$, respectavely. This symmetry is called *chiral symmetry*.

The Lagrangian density is invariant under both the flavour and chiral transformations. The conserved currents [39] are

$$j^A_\mu = \overline{q}_a \gamma_\mu (T^A)^a_b q^b, \quad \partial^\mu j^a_\mu = 0, \tag{3.14}$$

$$j^A_{5\mu} = \overline{q}_a \gamma_\mu \gamma_5 (T^A)^a_b q^b, \quad \partial^\mu j^a_{5\mu} = 0. \tag{3.15}$$

Since there is a mass term in the lagrangian, this symmetry is not an exact symmetry of QCD, as one can see from

$$\sum_j m_j \overline{q}_j q_j = \sum_{i,k} \overline{q}_{Rj} M_{jk} q_{Lk} + h.c., \tag{3.16}$$

where $M = diag(m_u, m_d)$. One added complication is the fact that one might expect the chiral symmetries to be spontaneously broken. Taking as an example [20], in the theory of superconductivity, the electrons in a superconducting metal can be influenced by an effective attractive potential due to the lattice phonons. Because of this attraction, a fraction of the eletrons can form "bound pairs". The vaccum of the phase is the one in which the bound pairs are all in the same state. This can be seen as the definition of a condensate. Thus, in

QCD, since quarks and antiquarks have strong attractive interactions, and in the approximation that they are massless, the energy necessary to create more quark-antiquark pairs is small. Thus one expects the existence of a condensate of quark-antiquark in the QCD vacuum. One has that

$$\langle 0|\, \overline{q}_{Rj} q_{Lk}\, |0\rangle = \Lambda^3 \delta_{jk}, \tag{3.17}$$

which transforms under $SU(2)_L \times SU(2)_R$. Performing a chiral transformation on the latter, one obtains

$$\langle 0|\, \overline{q}_{Rj} q_{Lk}\, |0\rangle = \Lambda^3 \delta_{jk} \to L_{jm} \langle 0|\, \overline{q}_{Rn} q_{Lm}\, |0\rangle\, R^{\dagger}_{nk} = \Lambda^3 \Sigma_{kj}, \tag{3.18}$$

where $\Sigma_{kj} = (LR^{\dagger})_{kj}$ is an SU(2) matrix. For $\Lambda \sim \Lambda_{QCD}$, Eq. (3.17) may be approximated by $\langle \overline{d}d \rangle = \langle \overline{u}u \rangle = \Lambda$ and the chiral symmetry is broken for $SU(2)_L \times SU(2)_R \to SU(2)_V$, with $L = R = V$. This symmetry is the isospin symmetry of the quark model. According to Goldstone, there sould exist three (pseudo)Goldstone bosons, one for each of the three broken generators. These excitations can be parametrized as

$$\Sigma(x) = e^{\frac{i2\pi(x)}{f}},\ \pi(x) = \pi^a(x) T_a, \tag{3.19}$$

where T_a are the generators of $SU(2)$ and $f \approx 93$ MeV is known as the *pion decay constant* [19, 38]. One can write the matrix π^a as

$$\pi = \frac{1}{\sqrt{2}} \begin{bmatrix} \frac{\pi^0}{\sqrt{2}} & \pi^+ \\ \pi^- & -\frac{\pi^0}{\sqrt{2}} \end{bmatrix}.$$

It is possible to identify each element of the matrix π with a real particle due to the fact that the latter transforms as an octet

$$\pi \to V \pi V^{\dagger}, \tag{3.20}$$

then restricting V to be an isospin rotation I_3, one can obtain the quantum numbers of each element of π.

The chiral lagrangian, including mass terms, reads

$$\mathcal{L}_C = \frac{f^2}{4} Tr[\partial \Sigma^{\dagger} \partial \Sigma] + \Lambda^2 f^2 \Big(\frac{c}{2\Lambda} Tr[M\Sigma] + h.c \Big) + ... \tag{3.21}$$

$$\approx Tr[\partial \pi^{\dagger} \partial \pi] + \frac{1}{2} f^2 \tilde{\Lambda} Tr[M\Sigma] + ... \tag{3.22}$$

where c is an unknwon constant and $\tilde{\Lambda} = c\Lambda$ [38]. The lagrangian presents the same approximate chiral symmetry of QCD which implies that the mass matrix transforms as $M \to VMV^{\dagger}$.

Expanding the chiral lagragian, it results in

$$\mathcal{L}_C^{\pi} \approx \frac{1}{2}\partial_\mu \pi^0 \partial^\mu \pi^0 + \partial_\mu \pi^- \partial^\mu \pi^+ - \tilde{\Lambda}(m_u + m_d)\frac{\pi^0\pi^0}{2} - \tilde{\Lambda}(m_u + m_d)\pi^-\pi^+ - \\ - \frac{\tilde{\Lambda}(m_u + m_d)}{48f^2}(\pi^0)^4 - \frac{\tilde{\Lambda}(m_u + m_d)}{12f^2}(\pi^-\pi^+)^2.$$

From the previous Lagrangian, the neutral pion can be described by a real scalar field with mass and self-coupling:

$$m_{\pi^0}^2 = \tilde{\Lambda}(m_u + m_d) \approx (135\ \text{MeV})^2, \tag{3.23}$$

$$\lambda_{\pi^0} = \frac{\tilde{\Lambda}(m_u + m_d)}{2f^2} \sim 1, \tag{3.24}$$

and the charged pions by a complex scalar field with mass and sef-coupling:

$$m_{\pi^+}^2 = \tilde{\Lambda}(m_u + m_d) + \text{ EM contribuitions} \approx (139\ \text{MeV})^2, \tag{3.25}$$

$$\lambda_{\pi^+} = \frac{\tilde{\Lambda}(m_u + m_d)}{3f^2} \sim 1. \tag{3.26}$$

3.2 Pion Properties

Since the neutral pion is not charged, it does not have eletromagnetic interations and thus, it cannot couple to the eletromagnetic field. But, experimentally, one knows that the neutral pions decays into two photons:

$$\pi^0 \to \gamma + \gamma. \tag{3.27}$$

This problem is understood in the view of QCD, since the neutral pion is composed by two charged quarks. This decay is possible due to the *axial anomaly*, or commonly known as *Adler-Bell-Jackiw Anomaly* [39, 40]. The current associated with the chiral symmetry of QCD, $j^{\mu 5}$, albeit classically conserved, $\partial_\mu j^{\mu 5} = 0$, is not conserved at the quantum level. Due to quantum corrections, one has that

$$\langle \partial_\mu j^{\mu 5} \rangle = -\frac{e^2}{16\pi^2}\tilde{F}_{\mu\nu}F^{\mu\nu}, \tag{3.28}$$

with $F_{\mu\nu}$ the eletromagnetic field strength tensor and $\tilde{F}_{\mu\nu} = (1/2)\epsilon_{\mu\nu\alpha\beta}F^{\alpha\beta}$. Thus, in the presence of an eletromagnetic field, the axial symmetry is explicitly broken and does not

depend on the fermion mass (as we will see below), which is not evident at the classical level [19, 39, 40][1].

To compute the pion decay width, we may consider first a toy model, corresponding to the QED Lagragian density with a Yukawa coupling bewteen a fermion ψ and a pseudoscalar ϕ:

$$\mathcal{L} = -\frac{1}{4}F_{\mu\nu}^2 - \frac{1}{2}\phi(D_\mu D^\mu - m_\pi^2)\phi + \overline{\psi}(i\gamma^\mu D_\mu - m)\psi + i\lambda\phi\overline{\psi}\gamma^5\psi. \tag{3.29}$$

The decay of the neutral pion into two photons, $\pi^0 \to \gamma\gamma$, then takes a contribution from the diagrams:

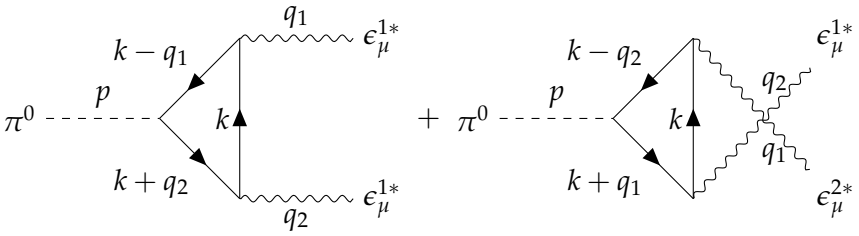

(3.30)

and the decay width is given by

$$\Gamma(\pi^0 \to \gamma\gamma) = \frac{\alpha^2}{64\pi^3}\lambda^2\frac{m_\pi^3}{m^2}. \tag{3.31}$$

To find the relation between this result and QCD, one considers the chiral lagragian without mass terms such that it preserves the full chiral symmetry. Considering an isospin doublet such as the proton and the neutron, $\Psi = (\psi_p, \psi_n)$, one can write a Lagragian invariant under $SU(2)_L \times SU(2)_R$

$$\begin{aligned}\mathcal{L} =& \frac{f^2}{4}Tr[\partial\Sigma^\dagger\partial\Sigma] + \overline{\Psi}_L i\gamma^\mu\partial_\mu\Psi_L + \overline{\Psi}_R i\gamma^\mu\partial_\mu\Psi_R - m_N\left(\overline{\Psi}_L\Sigma\Psi_R + \overline{\Psi}_R\Sigma^\dagger\Psi_L\right)\\ \approx& (-\frac{1}{2}\pi^0\nabla^\mu\nabla_\mu\pi^0 + ...) + \overline{\Psi}(i\gamma^\mu\partial_\mu - m_N)\Psi + i\frac{m_N}{f}\pi^0\overline{\Psi}\gamma^5\Psi + ...\end{aligned} \tag{3.32}$$

Matching with Eq. (3.29), one has that $m = m_N$ and $\lambda = m_N/f$, which gives the decay rate as

$$\Gamma(\pi^0 \to \gamma\gamma) = \frac{\alpha^2}{64\pi^3}\frac{m_\pi^3}{f^2}. \tag{3.33}$$

This leads to the prediction $\Gamma_\pi = 7.77$ eV [19] and experimentally the measured pion lifetime is $\tau \approx 8.4 \times 10^{-17}$ s, which corresponds to a width of $\Gamma_\pi \approx 7.83$ eV [41].

[1] This can be seen as the transformation being a symmetry of the Lagragian but not of the path integral.

The decay of the charged pion $\pi^+ \to e^+ + \nu_e$ has contribuition from the diagram

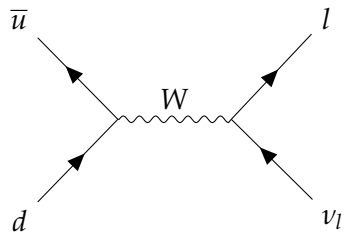

(3.34)

and the experimental value of the decay width is $(\Gamma_d)^{-1} \approx 2.6 \times 10^{-8}$ s [41]. One can also obtain the pion decay constant through this decay [19, 38].

Another electromagnetic process relevant to this work is the annihilation of charged pions, $\pi^+\pi^- \to \gamma\gamma$, and to study this process we may use scalar QED,

$$\mathcal{L} = -\frac{1}{4}F_{\mu\nu}^2 - |D_\mu\phi|^2 - \mu^2|\phi|^2, \tag{3.35}$$

where ϕ is a complex scalar field representing the charged pions. The corresponding annihilation rate is computed in Appendix C, yielding:

$$\Gamma_a^N \approx N\frac{\pi\alpha\hbar^2}{2\mu^2 Vc}, \tag{3.36}$$

where V is the volume of the region which contains N charged pions and α is the fine structure constant.

Chapter 4

Primordial Black Holes

Black holes that form from the collapse of stars, typically, have a mass of the order of the Sun's mass. However, we are interested in black holes that develop pion superradiant instabilities, with the superradiant condition imposing:

$$\alpha_\mu < \frac{1}{2} \implies M < 10^{12}\ \text{kg}. \tag{4.1}$$

These black holes cannot have a stellar origin. In 1971, Hawking predicted that gravitationally collapsed objects of mass 10^{-8} kg upwards could be formed as a result of fluctuations in the density of the early universe [5] and this is the kind of black hole we will be dealing with.

The study of these black holes provides new ways to probe the physics of the early universe, quantum gravity, gravitational collapse and high energy physics. For example, the evaporation of such black holes could change the details on baryogenesis and nucleosynthesis, could contribute to cosmic rays, cosmological and galactic $\gamma-$ray backgrounds [42, 43].

In this chapter, we will give a brief insight into the physics of primordial black holes.

4.1 Formation

The high density in the early Universe is necessary but not sufficient for primordial black holes to form. One needs density fluctuations such that overdense regions can eventually stop expanding and recollapse. There are several mechanisms in which primordial black holes could form such as phase transitions, collapse of cosmic loops and domain walls and bubble collisions [44].

It is expected that primordial black holes form if initial density fluctuations are large enough and a high density region collapses within its gravitational radius, i.e. the Schwarzchild radius [6]. These are known as primordial seeds which might form from inflation [45–51].

Inflation has an important role in the formation of primordial black holes. In the standard inflationary models, one makes the "slow-roll" assumptions (SRA) [52]:

$$\epsilon_\phi = \frac{1}{2}M_p^2\Big(\frac{V'(\phi)}{V(\phi)}\Big)^2 \ll 1, \quad \eta_\phi = M_p^2\Big(\frac{V''(\phi)}{V(\phi)}\Big) \ll 1, \tag{4.2}$$

where $V(\phi)$ is the potential for the inflaton scalar field. During inflation the scale factor grows exponentially,

$$a(t) \sim e^{Ht} \implies H \approx \text{constant}, \tag{4.3}$$

which leads to the Hubble parameter to be approximately constant. It is convinient to write the scale factor as a function of the conformal time, $d\tau = \int (dt/e^{Ht})$, as $a = -1/(H\tau)$. When studying the quantum fluctuations of the inflaton field [52],

$$\phi = \langle\phi\rangle + \delta\phi \quad \overset{\text{SRA}}{\Longrightarrow} \quad \Box\delta\phi = 0, \tag{4.4}$$

with $\delta\phi \ll \langle\phi\rangle$, one usually expands the fluctuations in Fourier modes, i.e. $\delta\phi \to \delta\phi_k$, and notices that the physical wavelength associated to a mode k is exponentially stretched by expansion during inflation:

$$\lambda = \frac{2\pi}{|k|}a. \tag{4.5}$$

At some point, this wavelength will be greater than the Hubble horizon which is pratically constant,

$$\lambda \gg H^{-1} \Leftrightarrow |k\tau| \ll 1. \tag{4.6}$$

One defines that a mode is inside the Hubble horizon when $|k\tau| \gg 1$ or is outside the Hubble horizon when $|k\tau| \ll 1$. The coefficents $\delta\phi_k$ can be written as

$$\delta\phi_k^{\pm} = \frac{1}{a}\Big(1 \mp \frac{i}{k\tau}\Big)e^{\mp ik}. \tag{4.7}$$

When a mode exits the horizon, the amplitude is $|\delta\phi_k^{\pm}| \approx H/k$ which approaches a constant value but when a mode is still deep inside the horizon, the amplitude is $|\delta\phi_k^{\pm}| \approx a^{-1}$ which decays exponentially. Thus, inflation not only stretches quantum fluctuations to superhorizons values and amplifies them to a constant value but also the amplitude of subhorizon

modes can be neglected in comparison to them.

One can define the power spectrum which characterizes the amplitude of the inflaton fluctuations as a function of k:

$$\mathcal{P}_\phi(k) = \frac{H^2}{2\pi k^3}. \tag{4.8}$$

The inflaton field is the dominant source of energy density during inflation, so pertubations in this field will lead to perturbations in the energy-momentum tensor and in the metric associated with the spacetime. These small quantum fluctuation will make the spacetime slightly inhomogeneous. The same process of stretching and amplification happens for the fluctuation in the metric and energy-momentum tensor. These fluctuations will later grow to form the structure of the universe that one sees today.

As for the case of the field fluctuations, one can define a power spectrum for the comoving curvature perturbation [52] $\mathcal{R}$

$$\mathcal{P}_\mathcal{R}(k) = \left(\frac{H}{\langle\dot{\phi}\rangle}\right)^2 \mathcal{P}_\phi(k), \tag{4.9}$$

which is common to express in terms of the dimensionless power spectrum

$$\Delta^2_\mathcal{R} = \left(\frac{H}{\langle\dot{\phi}\rangle}\right)^2 \left(\frac{H}{2\pi}\right)^2. \tag{4.10}$$

As mentioned above, during inflation the amplitude of the fluctuations, when outside the horizon, becomes constant. When inflation stops, the horizon starts to grows and the modes, once outside of it, will start to re-enter the horizon. This means that, eventually, all scales will re-enter the horizon and their amplitude will start to vary once again.

For a region to collapse to a primordial black hole, not only the fluctuation needs to be high enough but also the size of the region at the time it starts to collapse needs to be smaller than the particle horizon and greater than the Jeans length [53]. It needs to be smaller than the particle horizon such that it does not result in separated universes and it needs to be greater than the Jeans length such that the pressure cannot be sufficient to go against the gravitational collapse. These conditions already put constrains on the amplitude of the fluctuations [53]:

$$\delta_\mathcal{R} \sim 1. \tag{4.11}$$

From Eq. (4.8), it is expected that the spectrum of inflation perturbations to be *scale invariant*. While this is not entirely correct, since the field is slowly rolling, the field ϕ and associated

potential $V(\phi)$ values will be different for modes exiting the horizon at different times, one can measure deviatons from scale invariance by the spectral index n_s:

$$n_s - 1 \equiv \frac{d \ln \Delta^2_{\mathcal{R}}}{d \ln k} \simeq 2\eta_\phi - 6\epsilon_\phi. \tag{4.12}$$

From observations of the Cosmic Microwave Background (CMB) and to explain galaxy formation, one has that $\Delta^2_{\mathcal{R}} \sim 2 \times 10^{-9}$ and the measured spectral index is $n_s \approx 0.96 < 1$ [41]. As one can see from Eq. (4.12), the power spectrum takes the form $\Delta^2_{\mathcal{R}} \sim k^{n_s - 1}$ which means that the fluctuations grow with increasing scale. The constraint coming from galaxy formation would preclude the formation of primordial black holes on smaller scales. Thus, a possibility that includes the formation of primordial black holes to be possible is that the fluctuations should decrease with increasing scale, i.e. $n_s - 1 > 0$ on smaller scales, resulting:

$$\eta_\phi > 3\epsilon_\phi \quad \Longrightarrow \quad \left(\frac{V''(\phi)}{V(\phi)}\right) > \frac{3}{2}\left(\frac{V'(\phi)}{V(\phi)}\right)^2. \tag{4.13}$$

The field needs to be accelerating such that the previous condition is satisfied. This is possible in some inflationary scenarios [44–51, 54], where the scalar potential is designed to accomodate both small fluctuations on large CMB scales and large density fluctuations on small scales, as well as inflationary scenarios with multiple fields.

4.2 Mass and Spin

Normally, one assumes spherically symmetric, Gaussian fluctuations with a root-mean-square amplitude, which may depend on the mass, $\delta(M)$ and a equation of state $p = \gamma\rho$ with $0 < \gamma < 1$. One might expect a radiation equation of state ($\gamma = 1/3$) in the early universe after inflation but it could have deviated from this in some periods.

It is expected that primordial black holes would have a mass of the order of the particle horizon at their formation epoch, i.e. when fluctuations re-enter the horizon and collapse after inflation,

$$M(t) \approx \frac{c^3 t}{G}. \tag{4.14}$$

Thus, their masses span a very large range.

The fraction of regions of mass M which collapse to a black hole is [42]

$$\beta(M) \sim \delta(M) \exp\Big[-\frac{\gamma^2}{2\delta(M)^2}\Big]. \tag{4.15}$$

If the fluctuations were scale-invariant as seen before, the primordial black holes could have an extended mass function, where the number density of primordial black holes is given by:

$$\frac{dn}{dM} = (\alpha - 2)\frac{M}{M_*}^{-\alpha} M_*^{-2}\Omega_{\rm PBH}\rho_c, \tag{4.16}$$

where M_* is the current lower-cut-off on the mass spectrum due to evaporation, $\Omega_{\rm PBH}$ is the total density of the PBHs in units of the critical density and

$$\alpha = \left(\frac{1+3\gamma}{1+\gamma}\right) + 1. \tag{4.17}$$

Since, after inflation the universe enters in a radiation-dominated era in canonical scenarios, one has that $\gamma = 1/3$ and $\alpha = 5/3$. This means that the primordial black hole density goes as $M^{-1/2}$ since $n(M) \sim M^{-3/2}$ and $\rho(M) \sim M \times n(M)$ and so most of the primordial black holes density is contained in the smallest ones [44]. Once a primordial black hole is formed, its mass can vary due to accretion of the surrouding fluid. The accreted fluid will cross the Schwarzchild radius at the speed of light and so

$$\frac{dM}{dt} \sim \rho R_s^2 \sim t^{-2}M^{-2}, \tag{4.18}$$

which results in

$$M \sim \frac{t}{1 + \frac{t}{t_1}\left(\frac{t_1}{M_1} - 1\right)}, \tag{4.19}$$

where M_1 is the mass at t_1. If $M_1 = \eta t_1$ for $0 < \eta < 1$, then as t goes to infinity $M \sim M_1/(1-\eta)$. As one can see, the mass changes very little with time and one can make the approximation that $M \approx M_1$ [53].

Some recent studies have discussed the initial spin of primordial black holes. If black holes are formed in a radiation-dominated era, their spins should be very small $\tilde{a} \sim 10^{-2}$ [55, 56]. This is might be a consequence of considering Gaussian and spherical symmetric fluctuations. Now, if the inflaton field takes a long time to decay into radiation, it is possible to have an era dominated by inflaton matter between the end of inflation and reheating. Primordial BHs formed during this era should spin very fast and be near-extremal, $\tilde{a} \sim 1$ [57].

Primordial black holes should lose their spin due to Hawking evaporation at a rate comparable to the mass loss rate [58]. One characteristic of PBHs is that they are the only black holes that can be extremal since astrophysical BHs are bounded by the Thorne limit $a_{\rm lim} \approx 0.998$ from spinning up through accretion and as a primordial black hole tends to an extremal case, its lifetime could be reduced by 60% in comparinson with a non-spinning BH [59].

4.3 Constraints on Primordial Black Holes

4.3.1 Evaporation

As predicted by Hawking, a black hole emits thermal radiation with temperature

$$T = \frac{1}{8\pi M}, \tag{4.20}$$

assuming no charge and no rotation. Following [42, 60], a black hole emits particles with energy between E and $E + dE$ at a rate

$$d\dot{N}_\gamma = \frac{dE}{2\pi} \frac{\Gamma_s}{e^{E/T} - (-1)^{2s}}, \tag{4.21}$$

where s is the particle spin and Γ_s is its dimensionless absorption coefficient which in the high energy limit, $E \gg T$, $\Gamma_s \sim M^2$. At low energies, Γ_s will have a different form dependent on the particle spin. The total instantaneous flux emitted by a black hole is

$$\frac{dN}{dt} = \sum_i n_i \int_{\mu_i}^{\infty} \frac{d\dot{N}_\gamma}{dE} dE, \tag{4.22}$$

where n_i is the number of degrees of freedom per particle species i and μ is the particle rest mass. Multiplying Eq. (4.22) with the particle rest mass, one obtains the mass loss-rate of the black hole. Then, it is possible to obtain the threshold mass M_* for which black holes with mass $M < M_*$ have already evaporated today. This threshold mass is given by [61]

$$M_* \approx 5 \times 10^{11} \text{ kg}. \tag{4.23}$$

4.3.2 Bounds

The bounds that one presents here are based on the assumption that some fraction of dark matter is in the form of primordial black holes, i.e. $\Omega_{\text{PBH}} = f\Omega_{\text{DM}}$. The ideia that primordial black holes are a good condidate for dark matter comes from the early days in PBH research [43]. From a dynamical perspective, they behave just like any other form of dark matter.

There are many objects in the universe that can produce gamma rays. If one identifies all point-sources and extract their measured photon flux from the observed one, there will exist an isotropic gamma ray background (IGRB), also known as extragalactic diffuse photon background that fills the intergalactic medium. This background may have an origin from unresolved sources, being dark matter a possible one. The IGRB flux measured by four experiments (HEAO1+ballon [11], COMPTEL[12], EGRET[13] and FERMI-LAT[14]) are shown in Fig. 4.1.

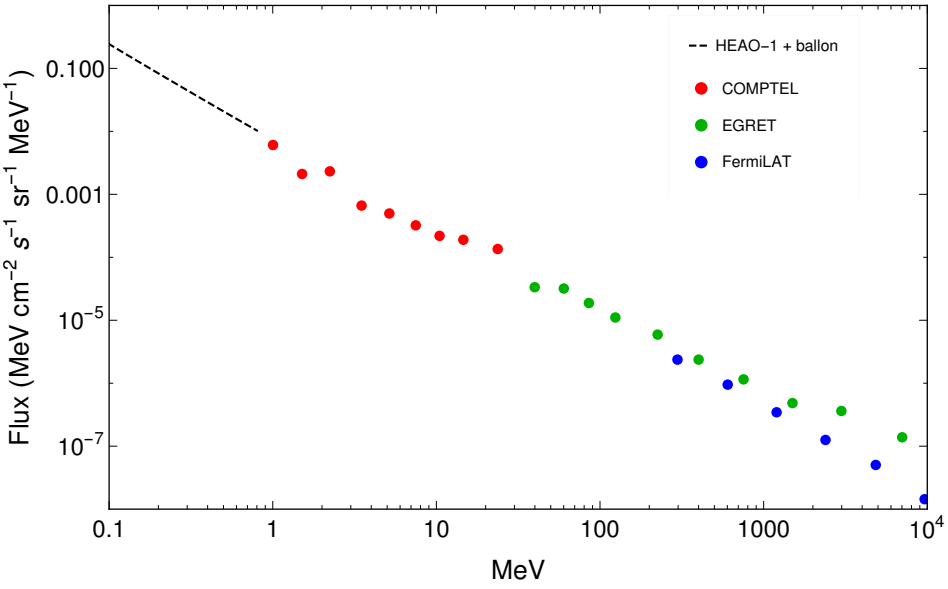

FIGURE 4.1: IGRB data as measured by four different experiments (HEAO1+ballon, COMPTEL, EGRET and FERMI-LAT).

Hawking and Page were one of the first people to use the diffuse extragalactic gamma ray background observations to constrain the mean cosmological number density of primordial black holes which are evaporationg at the current epoch at $\lesssim 10^4$ pc^{-3}, which corresponds to $\Omega_{\rm PBH} \lesssim 10^{-8}$ [42]. Later, some analysis have been made using the data from Fig. 4.1 to obtain a refinement of the previous constraint but all of them give $\Omega_{\rm PBH} \lesssim 10^{-8}$. A summary of the constraints on the abundance of PBH is presented in Fig. 4.2, where f is the fraction of dark matter in the form of primordial black holes [2].

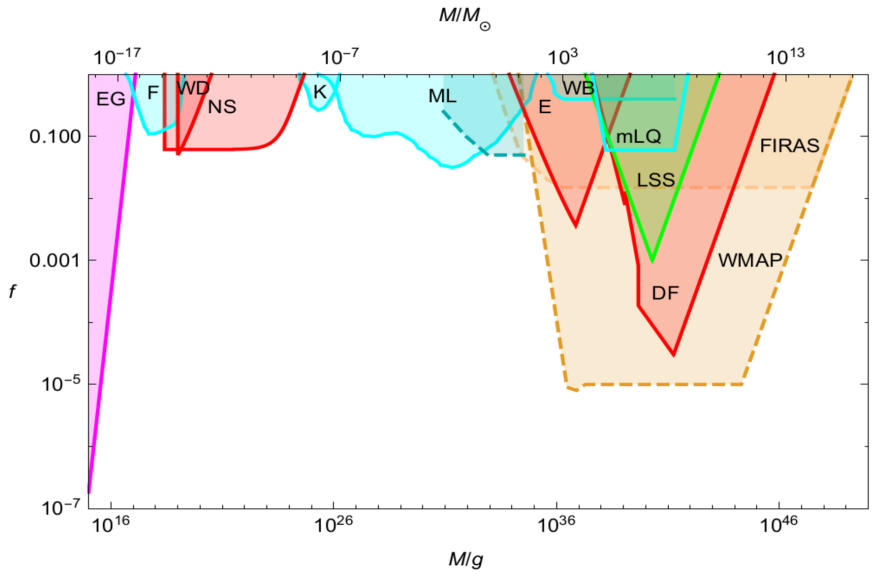

FIGURE 4.2: Observational constraints on the fraction of dark matter in primordial black holes for a wide range of primordial BH masses [2]. The constraints from the IGRB are represented in pink marked as EG.

Chapter 5

Pion Superradiant Instabilities of Primordial Black Holes

In the previous chapters, we have seen that superradiance can be a great tool to probe high energy physics and to study black hole properties. In this chapter, we will incorporate the result we obtained in Chapter 2 in the dynamics of a scalar field, which describes pions, to study the associated phenomenology. With the obtained results, we put constraints on the mass and spin of black holes that can generate superradiant instabilities associated with pions. We also discuss observational prospects of this phenomenon.

5.1 Neutral Pions

In the previous chapters, we have made a detailed analysis of the solutions of a massive scalar field in a Kerr spacetime. These solutions allow for the copious production of light bosonic particles in quasi-bound states around the BH, by extracting its rotational energy. In the non-relativistic regime[1], the spectrum of the bound state is Hydrogen-like:

$$\hbar\omega_n \approx \mu c^2\left(1-\frac{\alpha_\mu^2}{2n^2}\right) \tag{5.1}$$

and also, from the imaginary part of such frequency, ω_I, we obtained a growth rate

$$\Gamma_s(M,\tilde{a}) = \frac{2c^3}{MG}\left(\omega_I \frac{GM}{c^3}\right). \tag{5.2}$$

[1] In Chapter 2, $q = \sqrt{\omega^2-\mu^2}$ and in the non-relativistic regime $\bar{q} \ll 1$.

We will focus on the fastest mode $n = 2$ and $l = m = 1$, corresponding to a $2p-$pion cloud, since this state is populated exponentially faster than all others. We may also approximate the shape of this cloud by a torus with radii $\langle r \rangle = 5r_0$ and width $\Delta r = \sqrt{5}r_0$, where the "gravitational Bohr radius" is given by:

$$r_0 = \frac{\hbar}{\mu c \alpha_\mu} = \frac{\alpha_\mu^{-2}}{1+\sqrt{1-\tilde{a}^2}} r_+. \tag{5.3}$$

Thus, in the non-relativistic regime the pion cloud is localized far away from the horizon and we can neglect gravitational effects in the pion decay study. Another quantity which we will use is the root mean square (r.ms.) velocity which is given by $\sqrt{\langle v^2 \rangle} \approx (\alpha_\mu/2)c$ (See Appendix C).

Since we are using a scalar field to describe pions, we have to consider self-interactions as $(\lambda/4!)\phi^4$, with $\lambda \sim 1$. Due to self-interactions, the number of pions cannot grow arbitrarily large. When these are comparable to $(\mu^2/2)\phi^2$, their effect becomes relevant and the field reachs a critical value ϕ_c given by

$$\frac{\lambda}{4!}\phi^4 \sim \frac{\mu^2}{2}\phi^2 \implies \phi_c^2 \sim 12\frac{\mu^2}{\lambda}. \tag{5.4}$$

When the field reaches such a value within the cloud, the non-linear effects of self-interactions cause a gradual concentration of the pion field configuration which, eventually, leads to a dynamical collapse. The process consists in changing a pion from a superradiant state to a non-superradiant state where they can be absorbed back into the black hole. It leads to "bosenova" like explosions [29] that decrease the field value back to the linear superradiant regime where it can again grow up to the critical value. To this critical field value there is an associated critical number of pions which we define as N_c. Taking the value of the energy-momentum tensor associated with the pion field $T_{00} = \rho_\phi$, in the non-relativistic regime, the energy density can be written as $\rho_\phi = (\mu c^2 N)/V$, where $V = 50\pi^2 r_0^3$ is the volume of the cloud. Thus, in the critical case

$$N_c(\alpha_\mu) = 600\pi^2 \alpha_\mu^{-3}. \tag{5.5}$$

Taking as an example a black hole with $M_i = 5.5 \times 10^{11}$ kg, the critical number of neutral pions is $N_c \approx 3 \times 10^5$ and the cloud volume is $V_{cloud} \approx 7 \times 10^{-41}$ m^3. This gives a cloud density $\rho_\phi/c^2 \approx 9 \times 10^{17}$ kg/m^3 which is comparable to the nuclear density $\rho_n \approx 1.7 \times 10^{18}$ kg/m^3 (1 nucleon per 1 fm^3).

5.1.1 Allowed Primordial Black Holes

As mentioned in Chapter 3 , the neutral pion can decay into two photons,

$$\pi^0 \to \gamma + \gamma, \tag{5.6}$$

which is associated to a decay width Γ_d. While in a superradiant state, the number of neutral pions is governed by an effective rate $\Gamma_{eff} = \Gamma_s - \Gamma_d$, and thus, to have an effective production of neutral pions, the condition $\Gamma_{eff} > 0$ is necessary. This puts constraints on the possible black hole masses and spins.

We already have encountered an implicit mass constraint coming from the superradiant condition,

$$\alpha_\mu < \frac{1}{2} \implies M < \frac{\hbar c}{2\mu G} \tag{5.7}$$

which, for the neutral pion mass $\mu = 135\,\mathrm{MeV/c^2}$, it reads $M < 10^{12}$ kg. A stronger mass and spin constraints coming from $\Gamma_{eff} > 0$ is shown in Fig. 5.1.

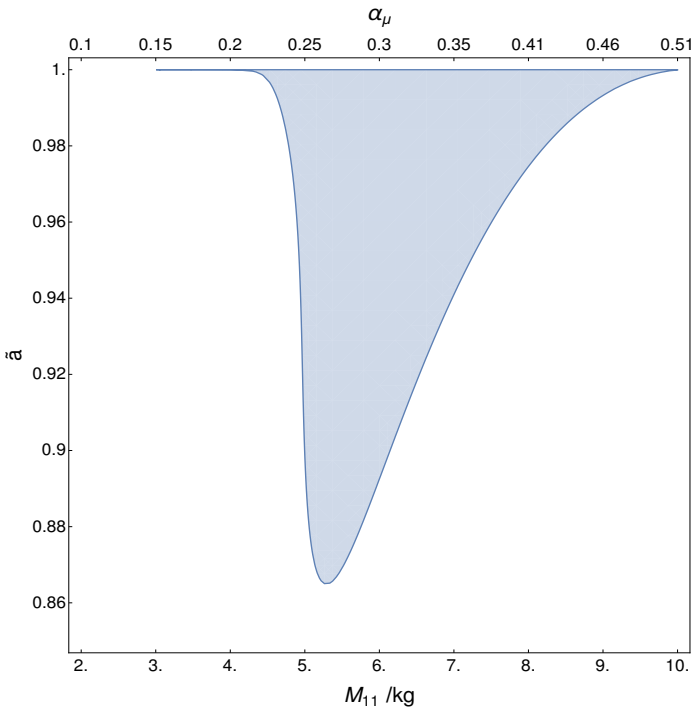

FIGURE 5.1: Regge plot with region (blue) for which black holes can produce effective superradiant instabilities for neutral pions.

As one can see, only black holes with high spin can effectively produce neutral pions from superradiant instabilities. It is expected that primordial black holes formed in a radiation-dominated era have low angular momentum [55, 56]. However, if they are formed in a

matter-dominated era [57, 62], e.g. if the inflation field takes a long time into decay to radiation and dominates the post-inflationary universe while oscillating about the minimum of its potential, then they could have a very high spin, in fact near extremal.

5.1.2 Dynamics

When a certain number N of pions is produced by a black hole, the change in the black hole mass and spin is $\delta M = \mu N$ and $\delta J = N\hbar$. Thus, defining $\delta k = k - k_f$ for $k = M,\ J,$ and $\tilde{a}$, it results in the following equations:

$$\frac{\delta M}{M} = \alpha_\mu \tilde{a} \frac{\delta J}{J}, \tag{5.8}$$

$$\frac{\delta \tilde{a}}{\tilde{a}} = 1 - \frac{1 - \frac{\delta J}{J}}{\left(1 - \alpha_\mu \tilde{a} \frac{\delta J}{J}\right)^2}. \tag{5.9}$$

Considering a black hole with initial mass M_i and initial spin $\tilde{a}_i$, we can compute how much mass and spin the black hole loses through superradiance, with the condition that the production of pions stops to be effective when $\Gamma_{eff}(M_f, \tilde{a}_f) = 0$. Taking as an example the black hole $M_i = 5.5 \times 10^{11}$ kg and $\tilde{a} = 0.99$, the change in mass is $\delta M \approx 3.5 \times 10^{10}$ kg and the change in spin is $\delta \tilde{a} \approx 0.12$.

We can also estimate how much time it takes for the condition $\Gamma_{eff} = 0$ to be attained, i.e. until the production of neutral pions becomes inefficient. Approximating the luminosity of the cloud as

$$L \approx 2 N_c \Gamma_d E_\gamma, \tag{5.10}$$

where $E_\gamma = (\mu c^2)/2$ is the energy of the photons, we estimate that the production of neutral pions is effective over a period

$$\Delta t \approx 1.4 \times 10^9 \text{ yr}. \tag{5.11}$$

We see that superradiant pion production and subsquent decay into photons shuts down before the present day and thus, before the primordial black holes evaporate $t_{ev} \sim 10^{10}$ yr. Since a significant loss of mass and spin through Hawking evaporation only occurs towards the end of its lifetime we may thus neglect, to a first approximation, the effects of evaporation.

Since the timescales Γ_s^{-1} and Δt are very different, i.e. $\Gamma_s^{-1} \ll \Delta t$, we may assume that the number of pions in the cloud is always near N_c, which varies adiabatically in time. While the superradiant regime is active, $\Gamma_{eff} > 0$, the dynamics is well described by the system of

equations:

$$\frac{d\alpha_\mu}{dt} = -\frac{\mu G}{\hbar c}\mu\Gamma_s N_c, \tag{5.12}$$

$$\frac{dJ}{dt} = -\hbar\Gamma_s N_c, \tag{5.13}$$

$$\frac{dN_\gamma}{dt} = 2\Gamma_d N_c, \tag{5.14}$$

where t is the cosmological time and N_γ is the number of photons coming from the decay of the neutral pions. Once $\Gamma_{eff} = 0$, the number of pions will decrease exponentially until it vanishes. We have solved the system with the help of Mathematica with the same initial black hole as before and we have obtained

$$\Delta t \approx 8 \times 10^8 \text{ yr}. \tag{5.15}$$

This result is slightly different from the estimated one because in this case the cloud luminosity increases with time, while in the estimate it was taken as constant. In Fig. 5.2 we show the time evolution of the normalized parameters, $\alpha_\mu^n(t) \equiv \alpha_\mu(t)/\alpha_\mu(0)$ and $J^n(t) \equiv J(t)/J(0)$, where $t^* = \hbar^2/(\mu^3 cG)$ is the natural scale of the system.

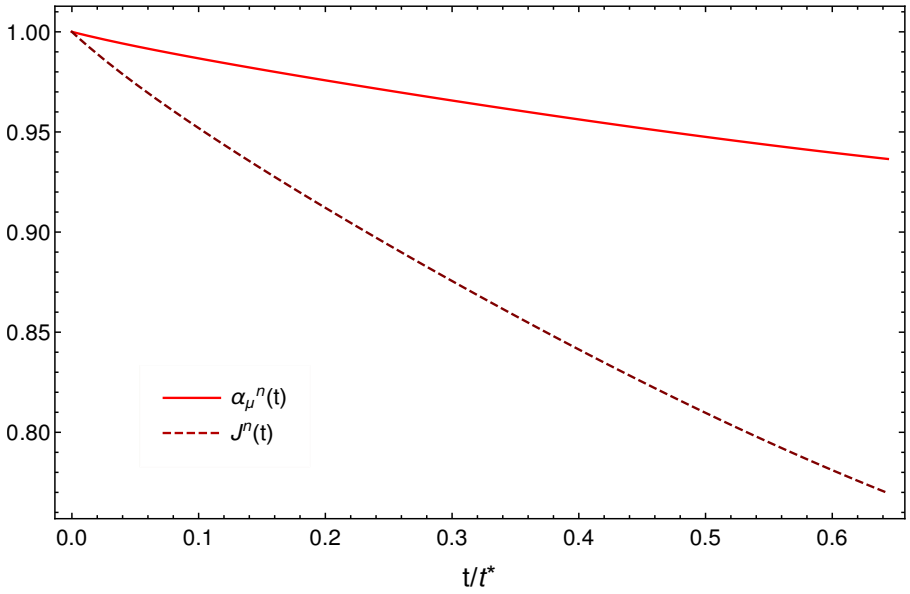

FIGURE 5.2: Dynamics of the normalized black hole parameters for a black hole with $M_i = 5.5 \times 10^{11}$ kg and $\tilde{a}_i = 0.99$ under superradiant instabilities of the neutral pion.

We can see that the black hole loses more angular momentum than mass and this could be predicted by Eqs. (5.8).

5.1.3 Photon Flux

From the dynamical system above which describes the evolution of the parameters of a black hole, one can compute the flux of photons that arise from this dynamics. We follow a similar procedure as [42]. We will consider the simple case where all primordial black holes have the same mass and spin. This has the advantage that they follow the same evolution and that the flux of photons today is a superposition of the photons emitted at all previous epochs. Since we can identify a certain flux of photons through its energy, we have that the total emission rate of photons per unit volume is the sum over all the emission rates of photons per unit volume at a given energy

$$\frac{dn_\gamma}{dt} = \sum_{E_\gamma} \frac{dn_\gamma}{dt}(E_\gamma). \tag{5.16}$$

The emission rate per unit volume for a given energy at cosmological time t is then:

$$\frac{dn_\gamma}{dt}(E_\gamma, t) = n_{\rm PBH}(t)\dot{N}_\gamma(E_\gamma, t), \tag{5.17}$$

where $n_{\rm PBH}$ is the number density of primordial black holes and the dot corresponds to a time derivative with respect to the cosmological time t. Observationaly, one measures the flux of photons in an interval of energy ΔE, which is associated to the resolution of the instrument in use. We use the approximation $\Delta E \approx E$, i.e. the flux per logarithmic energy scales [42]. Thus, one has that the flux can be written as

$$I = \frac{dI}{dE_\gamma}\Delta E_\gamma \approx \frac{dI}{dE_\gamma}E_\gamma. \tag{5.18}$$

It folllows that the emission rate of photons with energy E_γ is

$$\dot{N}_\gamma(E_\gamma) = E_\gamma \frac{d\dot{N}_\gamma}{dE_\gamma}(E_\gamma). \tag{5.19}$$

Defining the normalised spectral distribuition of photons as $\rho(E_\gamma)$, with $\int_0^\infty dE_\gamma \rho(E_\gamma) = 1$, the emission rate of photons with energy between E_γ and $E_\gamma + dE_\gamma$ is

$$d\dot{N}_\gamma = 2\Gamma_d N_c \rho(E_\gamma) dE_\gamma. \tag{5.20}$$

Due to the expansion of the Universe, both the number density of primordial black holes and the energy of photons at a cosmological time t will be seen today with redshift factors $(1+z)^{-3}$ and $(1+z)^{-1}$, respectively. The number density of primordial black holes can be written as $n_{\rm PBH}(t) = \Omega_{\rm PBH,0}(\rho_{0,c}/M)(1+z)^3$, where $\rho_{0,c}$ is the critical density of the universe today and $\Omega_{\rm PBH,0}$ is the abundance of primordial black holes today, the number density of

photons today can be given by (5.17) and takes the form

$$n_{\gamma,0}(E_{\gamma,0}) = 2\rho_{0,c}\Omega_{\mathrm{PBH},0}\Gamma_d E_{\gamma,0}\int_{t_{rec}}^{\Delta t} dt(1+z)\frac{N_c(t)}{M(t)}\rho(E_{\gamma,0}(1+z)), \tag{5.21}$$

where $t_{rec} \approx 400000$ yr is the time at which recombination started, $E_{\gamma,0}$ is the energy photon measured today and Δt is the already computed period where there is an effective production of pions. It was mentioned that primordial black holes could behave as cold dark matter before they evaporate. Thus, we will use this fact to relate the abundance of primordial black holes with the abundance of dark matter in the universe and we do this by using the relation $\Omega_{\mathrm{PBH},0} = f\Omega_{\mathrm{CDM},0}$, where f is the dark matter fraction in primordial black holes of mass M and spin $\tilde{a}$ [42, 63]. Even if we are dealing with black holes that are evaporating today, this fraction can be interpreted as the fraction that they would be if they had not evaporated.

From standard cosmology, inflation is followed by a radiation-dominated era which is followed by a matter-dominated era, and is now starting to be in a dark energy-dominated era. Since these primordial black holes were formed in the early universe, before the matter-dominated era, they started to emit photons before that era. Before recombination, all photons thermalise with the remaining cosmic plasma [52]. Hence, only the photons that were generated after reconbination, $t > t_{rec}$, will contribute to the extragalactic $\gamma-$ray background. Since $\Delta t < t_0$, where t_0 is the current age of the Universe, all photons are emitted in the matter-dominated era such that

$$1+z = \left(\frac{t}{t_0}\right)^{-2/3}. \tag{5.22}$$

To proceed with the calculations, we need to take notice of a detail in the kinematics of the neutral pion. Until now, we have been treating the pion as particle at rest. Even if the energy of the pion is $E_{\pi^0} \approx \mu + \mathcal{O}(\alpha_\mu^2)$, it possesses a r.m.s velocity $\sqrt{\langle v^2\rangle}$ as shown in a previous section. In the pion rest frame, the photons have energy $E_\gamma^r = \mu/2$ but in the cloud's frame $E_\gamma \to E_\gamma^r(1 \pm \alpha_\mu/2)$, in the non-relativistic regime.

We will consider two types of photon spectrum at emission, a simple monochromatic approximation (Delta Dirac function) and a Gaussian spectrum, both centered at E_γ^r, the Gaussian having a width $\sigma = E_\gamma^r\alpha_\mu/2$ and constituting a more realistic description.

The number density of photons for the monochromatic distribuition is given by

$$n_{\gamma,0}(E_{\gamma,0}, f) = 3f\rho_{0,c}\Omega_{\mathrm{CDM},0}\Gamma_d t_0\left(\frac{E_{\gamma,0}}{E_\gamma^r}\right)^{3/2}\frac{N_c(T)}{M(T)}\Theta(T - t_{rec})\Theta(\Delta t - T), \tag{5.23}$$

where T is such that $E_{\gamma,0}\left(\frac{T}{t_0}\right)^{-2/3} = E_\gamma^r$ and Θ is the Heaviside step function. The energy spectrum of photons will be limited since the flux (5.23) vanishes if a certain energy $E_{\gamma,0}$ leads

to $T < t_{rec}$ or $T > \Delta t$. Thus, the maximum energy is $E^0_{\gamma,\max} = E^r_\gamma \left(\frac{\Delta t}{t_0}\right)^{2/3}$ and the minimum energy is $E^0_{\gamma,\min} = E^r_\gamma \left(\frac{t_{rec}}{t_0}\right)^{2/3}$.

The number density of photons for the Gaussian distribuition is given by

$$n_{\gamma,0}(E_{\gamma,0}, f) = 2f\rho_{0,c}\Omega_{\mathrm{CDM},0}\Gamma_d E_{\gamma,0} \int_{t_{rec}}^{\Delta t} dt \left(\frac{t}{t_0}\right)^{-2/3} \frac{N_c(t)}{M(t)} \mathcal{N} \exp\left[\left(E_{\gamma,0}(t/t_0)^{-2/3} - E^r_\gamma\right)/(2\sigma^2)\right], \tag{5.24}$$

which needs to be computed numerically.

The flux of photons is defined as

$$I = \frac{c}{4\pi} n_{\gamma,0}, \tag{5.25}$$

in units of $\mathrm{s}^{-1}\mathrm{cm}^{-2}\mathrm{sr}^{-1}$. This flux is shown in Fig. 5.3 for an initial black hole with mass $M_i = 5.5 \times 10^{11}$ kg and spin $\tilde{a} = 0.99$ displaying both the monochromatic distribuition and the Gaussian distribuition.

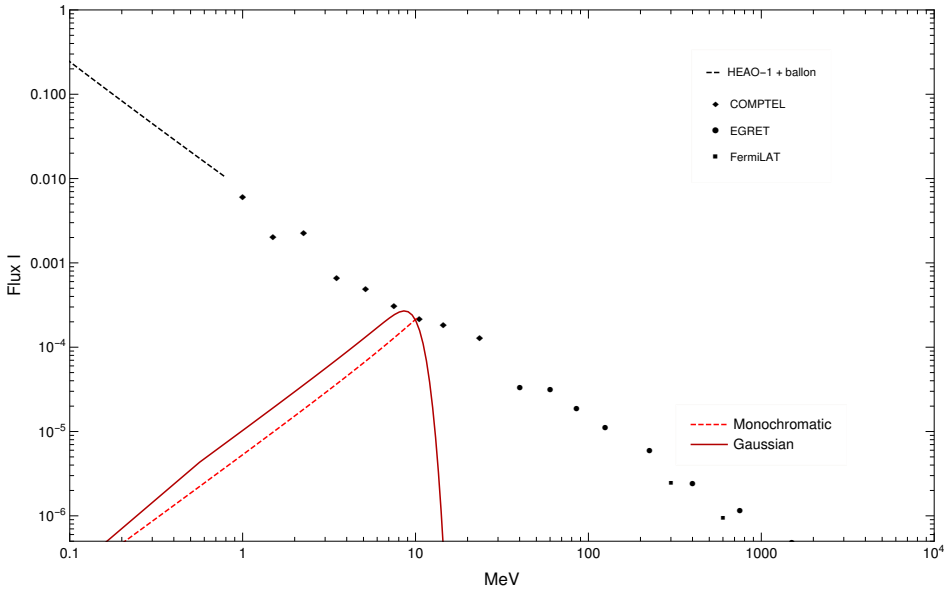

FIGURE 5.3: Photon flux from neutral pion decay in superradiant clouds, for a monochromatic (dashed curve) and Gaussian (solid curve) emission spectrum.

To compare with the data coming from the extragalactic $\gamma-$ray background (all black color data), we matched the maximum of each spectrum with the latter giving an upper bound on the fraction of dark matter in the form of primordial black holes with this mass and spin:

$$f \lesssim 10^{-7}, \quad \text{Gaussian} \tag{5.26}$$

$$\lesssim 7 \times 10^{-8}, \quad \text{monochromatic} \tag{5.27}$$

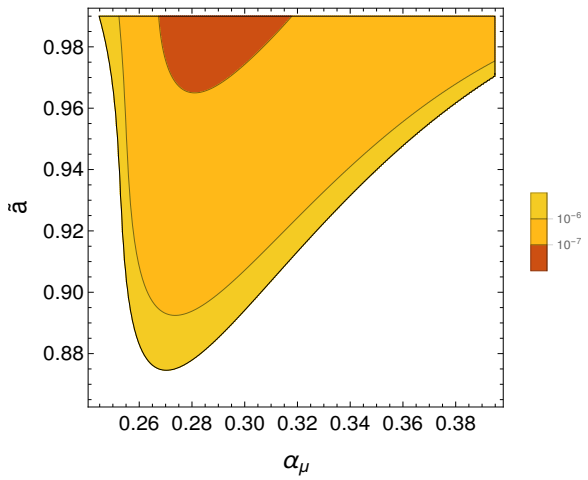

FIGURE 5.4: Upper bounds on the dark matter fraction f from neutral pion superradiance, showing contours for which $f < 10^{-7}$, $10^{-7} < f < 10^{-6}$ and $f > 10^{-6}$ given a monochromatic photon spectrum.

We have scanned the region where $\Gamma_{eff} > 0$ and computed the upper bound on f for each black hole inside it. This is shown in Fig. 5.4 and 5.5. The black holes that still agree with the constraints from evaporation are in the red regions of the plots.

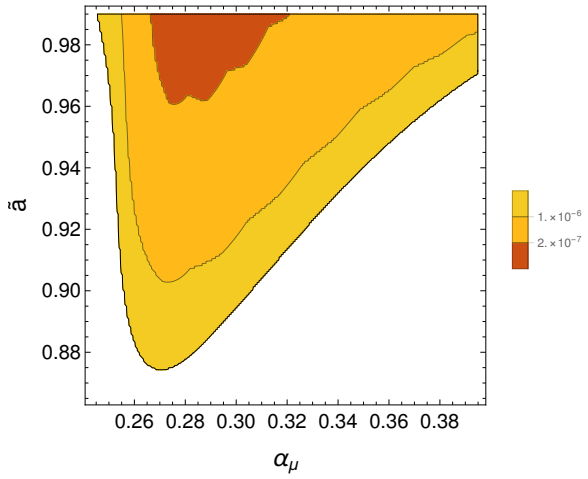

FIGURE 5.5: Upper bounds on the dark matter fraction f from neutral pion superradiance, showing contours for which $f < 2 \times 10^{-7}$, $2 \times 10^{-7} < f < 10^{-6}$ and $f > 10^{-6}$ given a Gaussian photon spectrum.

The non-smoothness of the contour plots is due to numerical errors.

5.2 Charged Pions

We now proceed the work by studying the charged pions in a analogous enviornment, considering its annihilation into two photons. Since the decay width of charged pions is smaller than the one from neutral pions, the condition $\Gamma_s > \Gamma_d^{\pm}$ gives a wider range for spin, going as low as $\tilde{a} \approx 0.1$ and for a different mass range as well. This is shown in Fig. 5.6.

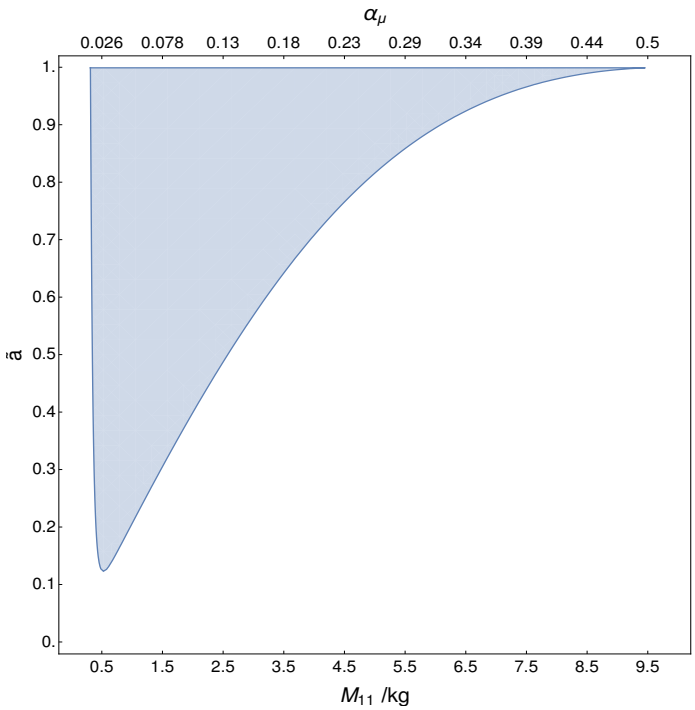

FIGURE 5.6: Regge plot with region (blue) for which black holes can produce effective superradiant instabilities for charged pions.

Using the same approach as in the case of neutral pions, we will describe charged pions as a scalar complex field. This field is allowed to have self-interactions as $(\lambda/4)(\phi^\dagger\phi)^2$. When these self-interactions are comparable to $\mu^2\phi^\dagger\phi$, their effect becomes relevant and the field reaches a critical value $|\phi_c|$ given by

$$\frac{\lambda}{4}|\phi|^4 \sim \mu^2|\phi|^2 \implies |\phi_c|^2 \sim 4\frac{\mu^2}{\lambda}. \tag{5.28}$$

and the same effect of "bosenova" like explosions happens when the field reaches such value.

Superradiant instabilities depend only on the mass of the particles, so antiparticles are treated equally and we consider that the number of positive charged pions N_+ is the same as of negative charged pions N_-, i.e. $N_+ = N_- = N$. In the non-relativistic limit, the energy density of the field is $\rho_\phi = (2\mu c^2 N)/V$, which comparing to T_{00} for a complex field, leads to the critical number of charged pions:

$$N_c(\alpha_\mu) = 200\pi^2\alpha_\mu^{-3}. \tag{5.29}$$

5.2.1 Allowed Primordial Black Holes

However, Fig. 5.6 is not the whole story. The charged pions produce photons also through annihilation,

$$\pi^+ + \pi^- \to \gamma + \gamma, \tag{5.30}$$

so that their number is governed by an effective rate Γ_{eff} which not only depends on Γ_s and $\Gamma_d^{\pm}$ but also on the annihilation rate Γ_a^N. However, the annihilation rate cannot be compared directly with Γ_s and $\Gamma_d^{\pm}$ since it depends on the number of charged pions present in the cloud. This annihilation rate is computed in Appendix C.

To know how superradiant instabilities can produce effectively charged pions, we need to look first at the dynamical equations which govern the evolution of a black hole under superradiant instabilities of such pions.

5.2.2 Dynamics

While in the superradiant regime, the dynamics can be well described by the following system of equations:

$$\frac{d\alpha_\mu}{dt} = -2\frac{\mu G}{\hbar c}\mu\Gamma_s N, \tag{5.31}$$

$$\frac{dJ}{dt} = -2\hbar\Gamma_s N, \tag{5.32}$$

$$\frac{dN}{dt} = (\Gamma_s - \Gamma_d)N - \Gamma_a N^2, \tag{5.33}$$

$$\frac{dN_\gamma}{dt} = 2\Gamma_a N^2, \tag{5.34}$$

where $\Gamma_a = \Gamma_a^N/N$ is the annihilation rate per particle. From Eq. (5.33) we can get a critical number at which $\frac{dN}{dt} = 0$:

$$N_c^a(\alpha_\mu, \tilde{a}) = \frac{\Gamma_s - \Gamma_d}{\Gamma_a} \approx \frac{\Gamma_s}{\Gamma_a}. \tag{5.35}$$

An effective production of charged pions, i.e. $\frac{dN}{dt} > 0$, leads to an upper bound on the number of pions $N < N_c^a$. We already have an upper bound on the number of pions coming from self-interactions but as we shall see, this upper bound is far greater than the one from annihilation, i.e. $N_c^a \ll N_c$. In Fig. 5.7 we show the regions in the black hole Regge plot for which $N_c^a > 1$, 10 and 50, with $N_c^a \geq 1$ to have at least one pair of opposite charge pions in the cloud surrouding the black hole.

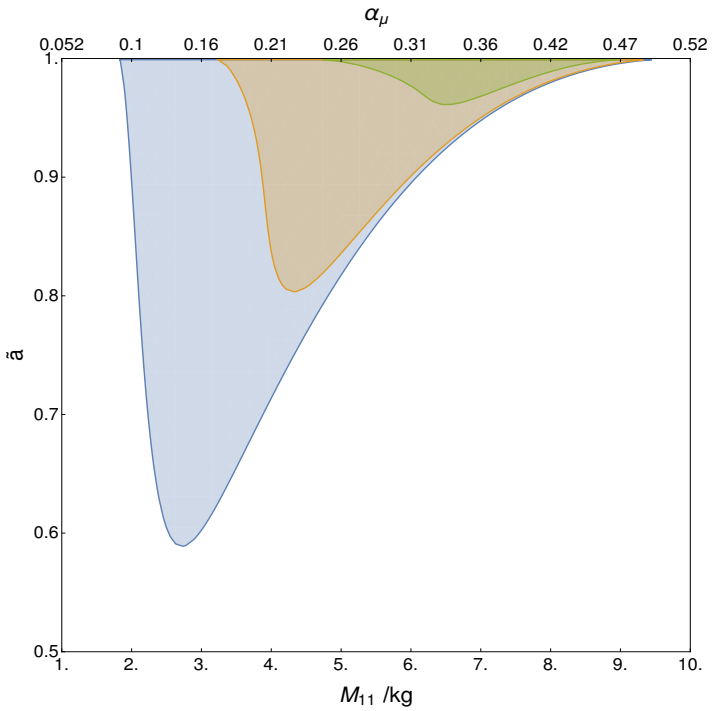

FIGURE 5.7: Regge plot with regions for which black holes can produce effective superradiant instabilities for charged pions considering now its annihilation. Regions where $N_c^a > 1$ (blue), $N_c^a > 10$ (brown) and $N_c^a > 50$ (breen) are shown.

Considering an initial black hole with mass $M_i = 5.5 \times 10^{11}$ kg and spin $\tilde{a}_i = 0.99$, we can approximate the luminosity of the cloud as $L \approx 2(N_c^a)^2 E_\gamma \Gamma_a$ with $E_\gamma = \mu c^2$, where $N_c^a \approx 50$. We estimate that the change in the black hole mass is $\delta M \approx 4.9 \times 10^{10}$ kg. Computing an estimated period where the production of charged pions is effective, the same way as for neutral pions, it yields:

$$\Delta t \approx 1.5 \times 10^{12} \text{ yr}. \tag{5.36}$$

The universe is $t_0 \approx 13.7 \times 10^9$ years old and so this process could be effective beyond the present day. Since black holes evaporate, the production of charged pions is sentenced to finish at the end of the black hole life, i.e. $\Delta t \approx \tau$, being τ the black hole lifetime. We will use the approximation that $\Delta t \approx 1$ Gyr. This approximation is justified by noticing that most of the black holes inside the colored regions in Fig. 5.7 have a mass $M < M_* \approx 5 \times 10^{11}$ kg smaller than the threshold mass for evaporation, i.e. they already have evaporated today. Considering that the process lasts ~ 1 Gyr is a good approximation since after that evaporation might have extracted a significant amount of spin from the black hole which might quench superradiance.

Fig. 5.8 shows the time evolution of the normalised black hole parameters $\alpha_\mu^n(t)$ and $J^n(t)$ for the previous initial black hole. We see that the same phenomenon happens where the

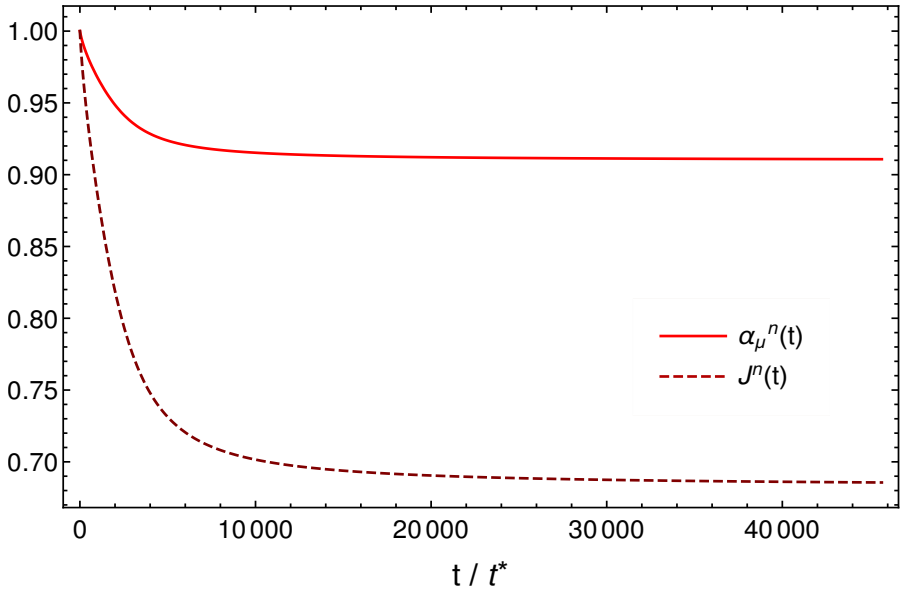

FIGURE 5.8: Dynamics of the normalized black hole parameters for a black hole with $M_i = 5.5 \times 10^{11}$ kg and $\tilde{a}_i = 0.99$ under superradiant instabilities of the charged pion.

change in angular momentum is greater than the mass change of the black hole. In this case, we obtained

$$\Delta t \approx 5.3 \times 10^{13} \text{yr}. \tag{5.37}$$

Again, from these dynamics, we will only consider the first 1 Gyr of the evolution and so the change in the mass and angular momentum will be very small.

5.2.3 Photon Flux

From Eq. (5.34), we have that the emission rate of photons with energy between E_γ and $E_\gamma + dE_\gamma$ is given by:

$$\frac{d\dot{N}_\gamma}{dE_\gamma} = 2\Gamma_a (N_c^a)^2 \rho(E_\gamma), \tag{5.38}$$

where $\rho(E_\gamma)$ is the same photon spectra as the neutral pion but with the difference that they are centered at $E_\gamma^r = \mu$. The number density of photons today is

$$n_{\gamma,0}(E_{\gamma,0}, f) = 2f\rho_{0,c}\Omega_{\text{CDM},0}E_{\gamma,0}\int_{t_{rec}}^{\Delta t} dt(1+z)\frac{\Gamma_a(t)(N_c^a(t))^2}{M(t)}\rho(E_{\gamma,0}(1+z)). \tag{5.39}$$

In the monochromatic case, we have:

$$n_{\gamma,0}(E_{\gamma,0}, f) = 3f\rho_{0,c}\Omega_{\text{CDM},0}\Gamma_d t_0 \left(\frac{E_{\gamma,0}}{E_\gamma^r}\right)^{3/2}\frac{\Gamma_a(T)(N_c^a(T))^2}{M(T)}\Theta(T - t_{rec})\Theta(\Delta t - T), \tag{5.40}$$

where T is such that $E_{\gamma,0}\left(\frac{T}{t_0}\right)^{-2/3} = E_\gamma^r$ and Θ is the Heaviside step function. In the Gaussian case, we have:

$$n_{\gamma,0}(E_{\gamma,0},f) = 2f\rho_{0,c}\Omega_{\mathrm{CDM},0}E_{\gamma,0}\int_{t_{rec}}^{\Delta t} dt\left(\frac{t}{t_0}\right)^{-2/3}\frac{\Gamma_a(t)(N_c^a(t))^2}{M(t)}\mathcal{N}\exp\left[\left(E_{\gamma,0}(t/t_0)^{-2/3} - E_\gamma^r\right)/(2\sigma^2)\right], \tag{5.41}$$

which needs to be computed numerically. The flux is shown in Fig. 5.9 for the two photon spectra. Matching the maximum of each flux with the observational data, we obtain that the

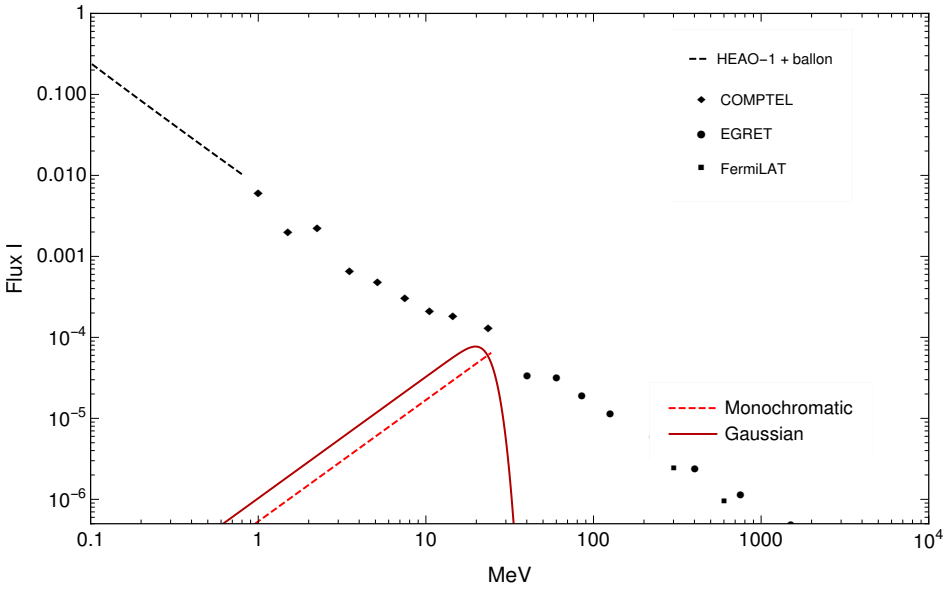

FIGURE 5.9: Photon flux from charged pion annihilation in superradiant clouds, for a monochromatic (dashed curve) and Gaussian (solid curve) emission spectrum.

upper bound on the fraction of dark matter in primordial black holes of this mass and spin is

$$f \lesssim 3\times 10^{-5}, \quad \text{monochromatic} \tag{5.42}$$

$$\lesssim 6\times 10^{-5}, \quad \text{Gaussian.} \tag{5.43}$$

Thus, we conclude that this process yields milder constrains on the primordial black hole fraction of dark matter than the process for neutral pions due to several reasons. The number of charged pions in the cloud is not significant enough to extract mass and angular momentum from the black hole in an appreciable amount of time, i.e. the loss rate of mass and angular momentum is too small compared to the one associated to the neutral pions, taking a larger amount of time to extract the same quantity of mass and angular momentum. Since the volume of the cloud depends on the black hole mass and it increases with the decrease of the same, the annihilation rate becomes smaller and smaller while the mass is decreasing.

This leads to a smaller number of events $\pi^+ + \pi^- \to \gamma + \gamma$, resulting in less photons emitted. Considering that $\dot{\alpha_\mu} \approx 0$, we have that $\dot{N}_c^a \approx \dot{\Gamma}_s/\Gamma_a < 0$, thus the number of charged pions in the cloud also decreases in time. However, we are dealing with a very small number of pions in the cloud, i.e. $N_c^a \sim \mathcal{O}(10)$, or even $N_c^a \sim \mathcal{O}(100)$, which may be an indicator that our classical treatment of the instability may not be appropriate.

5.3 Neutral and Charged Pions

5.3.1 Allowed Primordial Black Holes

From previous chapters, we analyzed separately the dynamics of neutral and charged pions. Now we assume that both are present in the cloud surrouding the black hole. We will assume that the neutral and charged pions do not interact with each other. This should be a good approximation when the number of pions is below the critical number, i.e. for cloud densities below the nuclear density. Thus, an effective production of pions is given independently whenever one of the condition is satisfied, i.e. there is an effective production of neutral pions when $\Gamma^0_{eff} > 0$ and there is an effective production of charged pions when $\Gamma^+_{eff} > 0$. We define any quantity with superscript 0 or $+$ by $A^{0,+} \equiv A(\alpha_\mu^{0,+})$, where $\alpha_\mu^{0,+} \equiv (\mu_{0,+}MG)/(\hbar c)$, being $\mu_{0,+}$ the mass of the neutral and charged pion, respectively.

The region where the production of pions is effective is shown in Fig. 5.10.

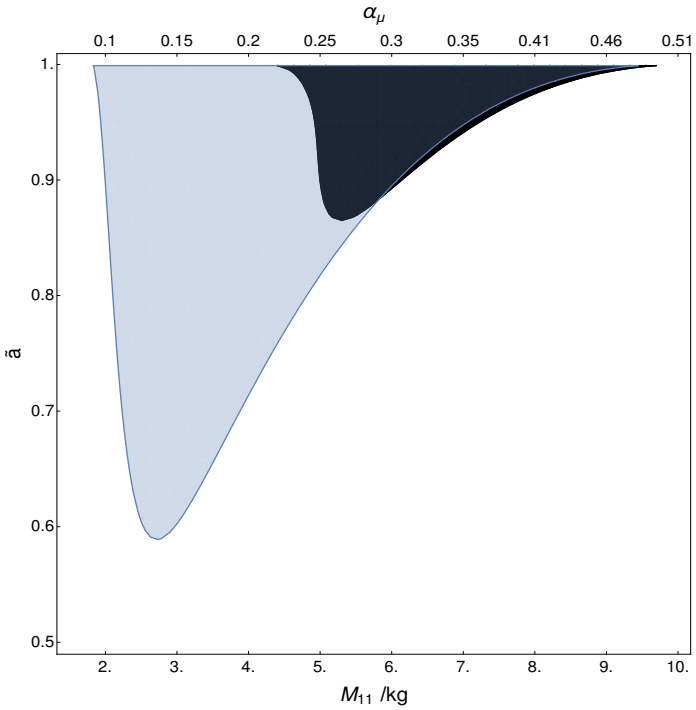

FIGURE 5.10: Regions where neutral (dark blue) and charged (blue) pion superradiant instabilities are efficient.

We expect that the evolution, dynamics and photon flux to be dominated by the neutral pions since in parametric regions where there is no neutral pion production, the number of charged pions is too small within the lifetime of the black hole to make signifcant changes in the black hole parameters. In regions where there are both neutral pions and charged pions, the number of neutral pions is always much larger than the number of charged pions by approximately four orders of magnitude.

5.3.2 Dynamics

While in the superradiant regime, the dynamics is well described by

$$\frac{d\alpha_\mu^0}{dt} = -\frac{\mu_0 G}{\hbar c}\mu_0\left(\Gamma_s^0 N_c^0 + 2\frac{\mu_+}{\mu_0}\Gamma_s\left(\frac{\mu_+}{\mu_0}\alpha_\mu^0\right)N_c^a\left(\frac{\mu_+}{\mu_0}\alpha_\mu^0\right)\right), \tag{5.44}$$

$$\frac{dJ}{dt} = -\hbar\left(\Gamma_s^0 N_c^0 + 2\frac{\mu_+}{\mu_0}\Gamma_s\left(\frac{\mu_+}{\mu_0}\alpha_\mu^0\right)N_c^a\left(\frac{\mu_+}{\mu_0}\alpha_\mu^0\right)\right), \tag{5.45}$$

$$\frac{dN_\gamma}{dt} = 2\Gamma_d N_c^0 + 2\Gamma_a^+ (N_c^a)^2. \tag{5.46}$$

Taking an initial black hole with mass $M_i = 5.5 \times 10^{11}$ kg and angular momentum $\tilde{a} = 0.99$, the full dynamics is depicted in Fig. 5.11. We compare with a system with only neutral pions. We see that the neutral pions dominate the evolution of the black hole over the charged pions as predicted ealier.

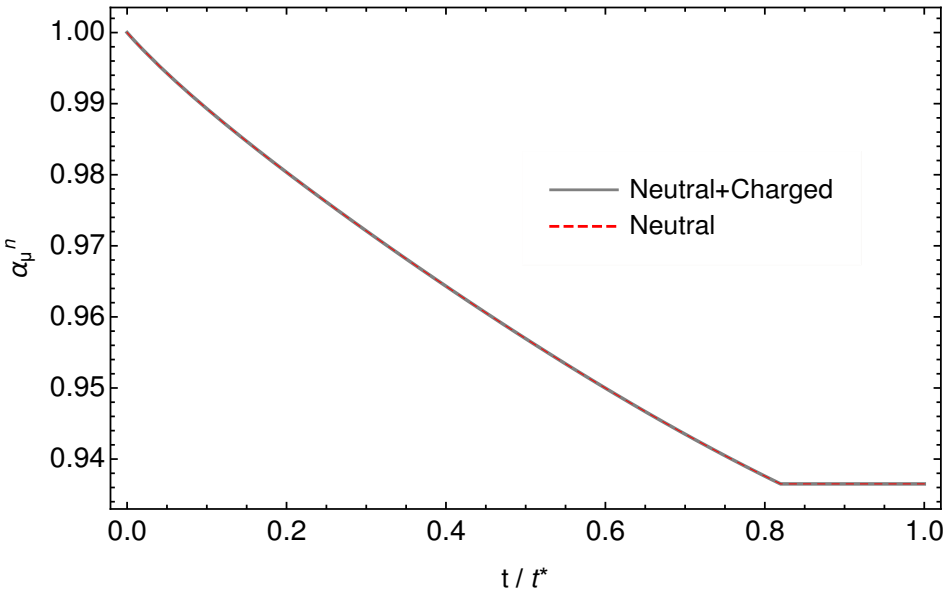

FIGURE 5.11: Dynamics of the normalized parameter α_μ^n considering the full system of pions (grey) and only considering the neutral pion (red).

We have that, from Eq. (5.46), the emission rate of photons with energy between E_γ and $E_\gamma + dE_\gamma$ is given by

$$\frac{d\dot{N}_\gamma}{dE_\gamma} = 2\Gamma_d N_c^0 \rho(E_\gamma - \frac{\mu_0}{2}) + 2\Gamma_a^+ (N_c^a)^2 \rho(E_\gamma - \mu_+). \tag{5.47}$$

Thus, number density of photons is

$$\begin{aligned} n_{\gamma,0}(E_{\gamma,0}) =& n_{\gamma,0}^0 + n_{\gamma,0}^+ \\ \approx& n_{\gamma,0}^0. \end{aligned} \tag{5.48}$$

The flux will be the same as the one from neutral pions and so the constraints will be the same as the ones form the neutral pion analysis.

5.4 Observational Prospects

Considering a Universe filled with matter and dark energy, $\Omega_{m,0} + \Omega_\Lambda = 1$, the Friedmann equation reads [52]

$$H^2 = \frac{\rho_m + \rho_\Lambda}{2M_p^2}, \tag{5.49}$$

where M_p is the Planck mass. Assuming an equation of state $p = \gamma\rho$, pressureless matter reads $\gamma = 0$ and, assuming that the cosmological constant is the right form of dark energy, dark energy reads $\gamma = -1$. It results that the energy density reads $\rho_\Lambda = \rho_{\Lambda,0}$ and $\rho_m = \rho_{m,0}(a/a_0)^{-3}$, where Eq. (5.49) becomes

$$H^2 = H_0^2\left(\Omega_{m,0}a^{-3} + \Omega_\Lambda\right). \tag{5.50}$$

The solution of this equation is the scalar factor

$$a(t) = \left(\frac{\Omega_{m0}}{1-\Omega_{m,0}}\right)^{1/3} \sinh^{2/3}\left(\frac{3}{2}H_0\sqrt{1-\Omega_{m,0}}t\right), \tag{5.51}$$

where we use $\Omega_{m,0} = 0.308$, $H_0 = 100h$ km s^{-1} Mpc^{-1} with $h = 0.678$ [41]. The redshift is given by

$$1 + z = \frac{a(t_0)}{a(t)}, \tag{5.52}$$

where we can obtain the age of the universe t_0 by solving $a(t_0) = 1$.

We are interested in what luminosity would a galaxy have if it contained some fraction of primordial BHs with superradiant pion clouds. We will only focus on the luminosity due to the decay of neutral pions since this process is the most prevalent one. We also have that, since the mass of the black hole does not vary much,

$$\begin{aligned}\frac{L_{\pi^0}}{L_{\pi^+}} &\approx \frac{\mu_0}{2\mu_+}\frac{\Gamma_d}{\Gamma_a}\frac{N_c^0}{(N_c^a)^2} \\ &\approx \text{constant.}\end{aligned} \tag{5.53}$$

Let us consider a galaxy (or galaxy cluster) of mass M_G which we assume to be dominated by dark matter. The number of primordial black holes in the galaxy is

$$N_{\text{PBH}} = f\frac{M_{\text{DM}}}{M_{\text{PBH}}} \sim f\frac{M_{\text{G}}}{M_{\text{PBH}}}, \tag{5.54}$$

where M_{PBH} the mass of the primordial black holes and f is the fraction of dark matter in primordial black holes of such mass. The luminosity associated with the decay of the neutral pions in superradiant clouds around such black holes into two photons is

$$L_{\pi^0} = 2f\frac{M_G}{M_{\text{PBH}}}\Gamma_d E_\gamma N_c^0 \quad \text{W}. \tag{5.55}$$

Using that $N_c = 4.6\times 10^{40} M_{\text{PBH}}^{-3}$ and defining $M_{\text{PBH}} = M_{11}\times 10^{11}$ kg and $f = f_7 \times 10^{-7}$, the luminosity can be rewritten as

$$L_{\pi^0} = 2.4\times 10^{25}\frac{f_7}{M_{11}^4}\frac{M_G}{M_\odot} \quad \text{W}, \tag{5.56}$$

where $M_\odot$ is the Sun's mass.

For example, for a black hole with mass $M_{11} = 5.5$ and angular momentum $\tilde{a} = 0.99$, we have emission of photons during $\Delta t = 8\times 10^8$ yr, according to Eq. (5.15). This corresponds to a redshift $z \approx 7$. The luminosity distance [52] can be written in termos of redshift as

$$d_L(z) = cH_0^{-1}\left(z + \frac{1}{2}(1-q_0)z^2 + ...\right), \tag{5.57}$$

where q_0 is the deceleration parameter of today. For a redshift of $z = 7$, it gives $d_L(z=7) \approx 2\times 10^5$ Mpc, which results in the flux density

$$\mathcal{F} = \frac{L_{\pi^0}}{4\pi d_L^2(z=7)} = 5.8\times 10^{-35} f_7 \frac{M_G}{M_\odot} \quad \text{Wm}^{-2}, \tag{5.58}$$

which, in more convinient units, where the photons have an average energy of $E_\gamma = 67.5$ MeV

$$\mathcal{F}_\gamma = 5.4 \times 10^{-28} f_7 \frac{M_G}{M_\odot} \quad \text{photon cm}^{-2}\,\text{s}^{-1}. \tag{5.59}$$

As we can see from the flux density, the heavier the galaxy, the greater its flux density. It is possible that exist there objects with mass $M_G \sim 10^{15} M_\odot$ at various redshifts. Two examples of such objects are the "El Gordo" [64], a galaxy cluster with a mass $M_{\text{EG}} = 3 \times 10^{15} M_\odot$ at a $z \approx 0.87$ redshift and a giant protocluster of galaxies [65] with a mass $M_{\text{PC}} \approx 4 \times 10^{15} M_\odot$ at a $z \approx 5.7$ redshift. We will consider that our object has a mass $M_G \sim 10^{15} M_\odot$. It follows that

$$L_{\pi^0} \approx 7 \times 10^{10} f_7 L_\odot, \tag{5.60}$$

where $L_\odot \approx 3.83 \times 10^{26}$ W is the solar luminosity. From the extragalactic $\gamma-$ray background constraints [59]. we see that the luminosity is bounded by

$$L_{\pi^0} < 7 \times 10^{10} L_\odot. \tag{5.61}$$

The flux density is given by

$$\mathcal{F}_\gamma \approx 5 \times 10^{-13} f_7 \quad \text{photon cm}^{-2}\,\text{s}^{-1}. \tag{5.62}$$

Presently, the most powerful instrument to observe $\gamma-$rays in the energy range 20 MeV - 300 GeV is the Fermi Gamma-ray Space Telescope. This instrument has a Point Source Sensitivity of $< 6 \times 10^{-9}$ photon cm^{-2} s^{-1} for energies > 100 MeV. For the case in study, the sensitivity is still not enough to detect the photons from superradiant pion clouds. One may, however, envisage a future γ-ray detector with an effective area of ~ 10 m^2, which could detect about one photon per year from neutral pion decay in superradiant clouds:

$$(5 \times 10^{-13}) \times (3 \times 10^8) \times (10^5) \approx 15 \text{ photons}. \tag{5.63}$$

Although much more difficult to detect, observing also the photons from charged pion annihilation would constitute a "smoking-gun" for pion superradiant instabilities around primordial black holes. This unique signal would correspond to two narrow emission lines from neutral pion decay and charged pion annihilation at energies $(\mu_0/2)/(1+z)$ and $\mu_+/(1+z)$, with an intensity ratio determined by the number of neutral and charged pions produced by superradiance, $N_{\pi^0}/N_{\pi^+} \sim 10^4$.

Chapter 6

Discussion and Conclusions

In this work, we studied superradiant instabilities of a massive spin-0 field in the vicinity of rotating black hole. This phenomenon happens when the real part of the frequency of the field satisfies $\omega_R < m\Omega_H$ and the instability growth rate is determined by the imaginary part ω_I of the frequency. One of the objectives was to obtain an analytical expression describing, with sufficient accuracy, the numerical results for the growth rate of the fastest superradiant bound state beyond the non-relativistic regime. Our pourpose was not precision physics but instead to have some analytical tool that could gives us, at least, the right order of magnitude of the growth rate. With this claim, the obtained expression agrees with numerical data within an average relative error up to $\lesssim 50\%$.

The second objective of this thesis was to study the dynamics and phenomenology associated with pions under superradiant instabilities. The purpose of this study was to constrain the mass and spin of the associated black holes. As we have seen, due to the pion mass, the black holes that could lead to superradiant instabilities of such particle belong in the class of primordial black holes, black holes that are formed in the early universe.

We began by making a separate analysis for the neutral pion and charged pion. In the neutral pion case, the condition to have an effective production of pions, $\Gamma_s > \Gamma_d$, also constrains the spin of a black hole and the possible values are not expected if these primordial black holes form in a radiation dominated era. However, they might be possible, if between the end of inflation and the beginning of recombination, there was some era dominated by pressureless matter. When studying the properties of the cloud, we noticed that the cloud density is of the order of the nuclear density and when the density becomes greater than the nuclear density, "bosenova"-like explosions take place. Assuming that some fraction of dark matter can be in the form of primordial black holes in the relevant mass and spin range, $\Omega_{\rm PBH} = f\Omega_{\rm DM}$, we obtained that this fraction is $f \lesssim 10^{-7}$ for a certain group of black holes, which is

comparable to the constraints coming from evaporation[1]. In the charged pion case, we made the same analysis as before but the condition to have an effective production of pions is $\Gamma_s > N\Gamma_a$, which depends on the number of pions in the cloud. We have found that superradiant charged pion production can occur for lower BH spins that for the neutral pions. However, the number of pions in the cloud is not significant enough to have an important impact on the black hole dynamics in the span of its lifetime and since we are using a classical description of the field, this approximation may not be appropriate due to the small occupation numbers obtained for the leading superradiant bound state. Finally, we considered the system with neutral and charged pions and noticed that the dynamics is governed by the neutral pion and the system can be approximated by a system with neutral pions only.

Finally, we have estimated the luminosity of a point source object at large redshift containing a small fraction of dark matter in the form of primordial black holes with active superradiant pion clouds. We concluded that this is in principle too low to be detected with current technology, but neverthless estimated the size of a future γ-ray telescope capable of finding such a "smoking-gun" of primordial BH superradiance.

[1] Photons emitted through Hawking evaporation also contribute to the IGRB

Appendix A

Scalar field properties in superradiant bound states

The Lagrangian density of a free real scalar field ϕ [18] is given by

$$\mathcal{L} = -\frac{1}{2}\partial_\mu\phi\partial^\mu\phi - \frac{1}{2}\mu^2\phi^2, \tag{A.1}$$

and from Noether's Theorem, the associated enery-momentum tensor [18] is

$$T_{\mu\nu} = \partial_\mu\phi\partial_\nu\phi - \frac{1}{2}\eta_{\mu\nu}\Big(\partial_\alpha\phi\partial^\alpha\phi + \mu^2\phi^2\Big). \tag{A.2}$$

We can approximate the kinetic term in Eq. (A.1) as

$$\partial_\mu\phi\partial^\mu\phi = -(\dot{\phi})^2 + (\nabla\phi)^2 \approx -(\dot{\phi})^2, \tag{A.3}$$

within a non-relativistic superradiant cloud where $\dot{\phi} \sim \mu\phi$ and $|\nabla\phi| \sim \alpha_\mu\mu\phi$. Thus, the energy density can be written as

$$\begin{aligned}\rho_\phi = T_{00} &\approx (\dot{\phi})^2 + \frac{1}{2}\Big(-(\dot{\phi})^2 + \mu^2\phi^2\Big) \\ &= \frac{1}{2}\Big((\dot{\phi})^2 + \mu^2\phi^2\Big).\end{aligned} \tag{A.4}$$

Since the field varies in time as $\phi \propto e^{-i\omega t}$ and is real, it results in

$$\rho_\phi = \mu^2\phi^2, \tag{A.5}$$

where we used $\omega \approx \mu$.

The Lagrangian density for a complex scalar field [18] is given by

$$\mathcal{L} = -\partial^\mu \phi \partial_\mu \phi^* - \mu^2 \phi \phi^*, \tag{A.6}$$

and from Noether's theorem, the associated enery-momentum tensor [18] is

$$T_{\mu\nu} = \partial_\mu \phi^* \partial_\nu \phi + \partial_\mu \phi \partial_\nu \phi^* - \eta_{\mu\nu}\Big(\partial^\alpha \phi \partial_\alpha \phi^* + \mu^2 \phi \phi^*\Big). \tag{A.7}$$

Using the same approximation, in the non-relativistic regime, the energy density reads

$$\begin{aligned} \rho_\phi &\approx \dot{\phi}\dot{\phi}^* + \mu^2 \phi \phi^* \\ &\approx 2\mu^2 \phi \phi^*. \end{aligned} \tag{A.8}$$

In the far region of the Kerr spacetime, the radial differential equation takes the same form as for the Hydrogen atom. The radial part for a $2p$-cloud takes the form

$$R(r) = \frac{1}{\sqrt{3}}(2r_0)^{-3/2}\Big(\frac{r}{r_0}\Big)e^{r/(2r_0)}, \tag{A.9}$$

where $r_0 = \hbar/(\mu c \alpha_\mu)$ and we obtain that

$$\langle r \rangle = \int_0^\infty r \times r^2 |R(r)|^2 dr = 5r_0, \tag{A.10}$$

$$\Delta r = \sqrt{\langle r^2 \rangle - \langle r \rangle^2} = \sqrt{5} r_0. \tag{A.11}$$

To compute the velocity, we notice that $-\mu(\alpha_\mu^2/8) = \langle H \rangle = \langle |p|^2/(2\mu) \rangle + \langle V(r) \rangle$ and $|v|^2 = |p|^2/\mu^2$, where $V(r) \sim \alpha_\mu^2/r$ and H is the Hamiltonian. It results in

$$\langle |v|^2 \rangle = \frac{2}{\mu}\Big(\langle H \rangle - \langle V(r) \rangle\Big) = \frac{1}{4}\alpha_\mu^2 c^2. \tag{A.12}$$

For a torus with radii $a = \langle r \rangle$ and width $c = \Delta r$, its volume is $V_{cloud} = 2\pi^2 c^2 a = 50\pi^2 r_0^3$. In natural units

$$\begin{aligned} N_c \sim \mu^3 \times V_{cloud} &= 50\pi^2 \mu^3 \times \Big(\mu \alpha_\mu\Big)^{-3} \\ &= 50\pi^2 \alpha_\mu^{-3}. \end{aligned} \tag{A.13}$$

Appendix B

Useful Gamma-function properties

Here we derive some useful mathematical results, based on the following properties of gamma-functions:

1. $\Gamma(z) = (z-1)!$
2. $\psi(z+n) = \frac{1}{n-1+z} + ... + \frac{1}{1+z} + \frac{1}{z} + \psi(z)$
3. $\lim_{z\to 0} \frac{\psi(z)}{\Gamma(z)} = -1$
4. $\lim_{z\to 0} \Gamma(z) = \infty$
5. $\lim_{z\to 0} \frac{\Gamma(-nz)}{\Gamma(-mz)} = \frac{m}{n}$

where m, n are non-negative integers and $\psi(z) = \Gamma'(z)/\Gamma(z)$.

The first results reads:

$$\lim_{z\to -n} \frac{\psi(z)}{\Gamma(z)} = \lim_{w\to 0} \frac{\psi(w-n)}{\Gamma(w-n)} \tag{B.1}$$

$$= \lim_{w\to 0} \frac{\prod_{i=1}^{n}(w-i)}{\Gamma(w)} \Big[-\sum_{i=1}^{n} \frac{1}{w-i} + \psi(w) \Big] \tag{B.2}$$

$$= \lim_{w\to 0} \frac{\psi(w)}{\Gamma(w)} \prod_{i=1}^{n}(w-i) \tag{B.3}$$

$$= (-1)^{n+1} n! \tag{B.4}$$

The second result is:

$$\frac{\Gamma(-2l-1)}{\Gamma(-l)} = \lim_{\epsilon\to 0}\frac{\Gamma(-2l-2\epsilon-1)}{\Gamma(-l-\epsilon)} \tag{B.5}$$

$$= \lim_{\epsilon\to 0}\Big(\lim_{z\to -\epsilon}\frac{\Gamma(2z-2l-1)}{\Gamma(z-l)}\Big) \tag{B.6}$$

$$= \lim_{\epsilon\to 0}\Big(\lim_{z\to -\epsilon}\frac{\Gamma(2z)}{\prod_{i=1}^{2l+1}(2z-i)}\frac{\prod_{j=1}^{l}(z-j)}{\Gamma(z)}\Big) \tag{B.7}$$

$$= \lim_{\epsilon\to 0}\Big(\frac{\Gamma(-2\epsilon)}{\prod_{i=1}^{2l+1}(-2\epsilon-i)}\frac{\prod_{j=1}^{l}(-\epsilon-j)}{\Gamma(-\epsilon)}\Big) \tag{B.8}$$

$$= \frac{1}{2}(-1)^{l+1}\frac{l!}{(2l+1)!}. \tag{B.9}$$

The third result reads:

$$\frac{\Gamma(l+1-y)}{\Gamma(-l-y)} = \lim_{z\to -y}\frac{\Gamma(l+1+z)}{\Gamma(-l+z)} \tag{B.10}$$

$$= \lim_{z\to -y}(z+l)(z+l-1)...(z+1)z(z-1)...(z-l) \tag{B.11}$$

$$= (-1)^l x\prod_{k=1}^{l}(k^2-y^2). \tag{B.12}$$

Appendix C

Charged Pion Annihilation Rate

C.1 Matrix element $\mathcal{M}_{fi}$

Expanding the Lagragian density in Eq. (3.35), we see that the part corresponding to photon interactions is

$$\mathcal{L}_{int} = -A_\mu J^\mu - e^2 A_\mu A^\mu \phi\phi^\dagger \tag{C.1}$$

where $J_\mu = ie(\phi\partial_\mu\phi^\dagger - \phi^\dagger\partial_\mu\phi)$ and the corresponding vertices are

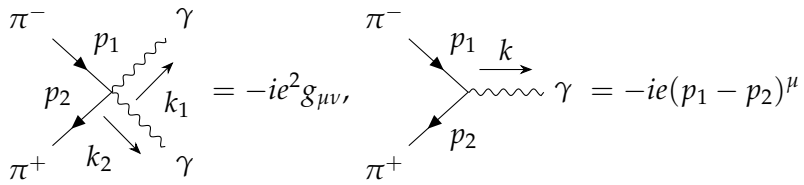

The diagrams to compute the matrix element are, up to order $\mathcal{O}(e^3)$,

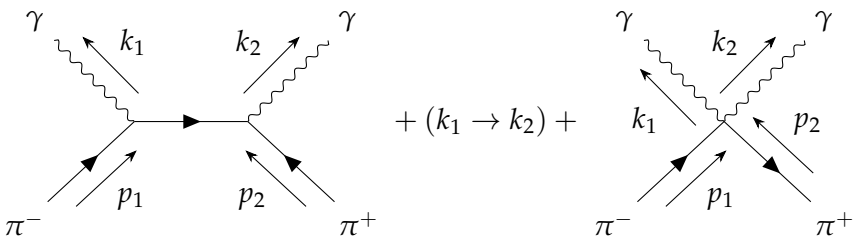

Following the Feynman rules to compute the matrix element, then

$$i\mathcal{M} = -ie^2\left[\frac{(2p_1-k_1)^\mu\epsilon_\mu(k_1)(2p_2-k_2)^\nu\epsilon_\nu(k_2)}{\mu^2-t}+\frac{(2p_1-k_2)^\mu\epsilon_\mu(k_2)(2p_2-k_1)^\nu\epsilon_\nu(k_1)}{\mu^2-u}\right. \tag{C.2}$$

$$\left.+\,2\epsilon_\mu(k_1)\epsilon^\mu(k_2)\right] = \tag{C.3}$$

$$= -ie^2\epsilon_\mu(k_1)\epsilon_\nu(k_2)\left[\frac{(2p_1-k_1)^\mu(2p_2-k_2)^\nu}{\mu^2-t}+\frac{(2p_1-k_2)^\nu(2p_2-k_2)^\mu}{\mu^2-u}+g_{\mu\nu}\right] = \tag{C.4}$$

$$= -ie^2\epsilon_\mu(k_1)\epsilon_\nu(k_2)\mathcal{M}^{\mu\nu}. \tag{C.5}$$

We see that the Ward identities are satisfied $k_\mu^1\mathcal{M}^{\mu\nu} = k_\mu^2\mathcal{M}^{\mu\nu} = 0$ and using the fact that $p_1+p_2 = k_1+k_2$ and $k_i\cdot\epsilon^i = 0$, $\mathcal{M}^{\mu\nu}$ can be rewritten as

$$\mathcal{M}^{\mu\nu} = 2\left[2\frac{p_1^\mu(k_1-p_1)^\nu}{\mu^2-t}+2\frac{p_1^\nu(k_2-p1)^\mu}{\mu^2-u}+g^{\mu\nu}\right]. \tag{C.6}$$

Averaging over photon polarizations and using $\sum_\lambda \epsilon^{*\mu}_{(\lambda)}(k)\epsilon^{(\lambda)\nu}(k) = g^{\mu\nu}$ one obtains

$$\langle|\mathcal{M}|^2\rangle_{pol} = \frac{1}{4}\sum_{\lambda\lambda'}\langle|\mathcal{M}|^2\rangle = \frac{1}{4}\mathcal{M}^*_{\mu\nu}\mathcal{M}^{\mu\nu}. \tag{C.7}$$

After some algebra, we have that

$$\mathcal{M}^*_{\mu\nu}\mathcal{M}^{\mu\nu} = 16\left[1+\frac{\mu^2t}{(\mu^2-t)^2}+\frac{\mu^2u}{(\mu^2-u)^2}+\frac{p_1\cdot k_1+\mu^2}{\mu^2-t}+\frac{p_1\cdot k_2+\mu^2}{\mu^2-u}\right. \tag{C.8}$$

$$\left.+\,2\frac{(p_1\cdot k_1+\mu^2)(p_1\cdot k_2+\mu^2)}{(\mu^2-t)(\mu^2-u)}\right. . \tag{C.9}$$

Taking $2p_1\cdot k_1 = t-\mu^2$ and $2p_1\cdot k_2 = u-\mu^2$ and after some algebra

$$\langle|\mathcal{M}|^2\rangle_{pol} = 2e^4\frac{5\mu^8-4(u+t)\mu^6+\mu^4(u^2+t^2)+u^2t^2}{(\mu^2-t)^2(\mu^2-u)^2}. \tag{C.10}$$

In the non-relativistic regime, $s \approx 4\mu^2$. Using the equality $s + t + u = 2\mu^2$ and $t \approx -\mu^2$, it leads to

$$\langle |\mathcal{M}|^2 \rangle_{pol} \approx 2e^4 = 32\pi^2\alpha^2, \tag{C.11}$$

where α is the fine structure constant.

C.2 Cross section

Considering that we have the scattering $1 + 2 \rightarrow 3 + 4$ of two particles, the initial state is $|i\rangle = |\pi^-(p_1)\pi^+(p_2)\rangle_{in}$ and the final state is $|f\rangle = |\gamma(p_3)\gamma(p_4)\rangle_{out}$, where in the end of the calculation we consider the particles as being charged pions and photons. The probability of transition from one state to another is

$$P_{fi} = \frac{|{}_{out}\langle f|i\rangle_{in}|^2}{\langle f|f\rangle \langle i|i\rangle} \tag{C.12}$$

where ${}_{out}\langle f|i\rangle_{in} = {}_{in}\langle f| S |i\rangle_{in} = (2\pi)^4\delta(p_f - p_i)i\mathcal{M}_{fi}$. Defining the states as 1-particle states, their normalization is $\langle p|p\rangle = 2E_pV$ and the transition probability is

$$P_{fi} = \frac{TV(2\pi)^4\delta(p_f - p_i)|\mathcal{M}_{fi}|^2}{(2E_{p_1}V)(2E_{p_2}V)(2E_{p_3}V)(2E_{p_4}V)}. \tag{C.13}$$

Summing over the final states, we have that

$$P_i = \frac{T}{V}\frac{(2\pi)^4}{4E_{p_1}E_{p_2}}\int \frac{d^3p_3}{(2\pi)^3 2E_{p_3}}\frac{d^3p_4}{(2\pi)^3 2E_{p_4}}\delta(p_f - p_i)|\mathcal{M}_{fi}|^2 \tag{C.14}$$

The rate of the transition is

$$\frac{P_i}{T} = f_{inc} \times \sigma_i \tag{C.15}$$

where the flux of incident particles is $f_{inc} = \frac{|v_1 - v_2|}{V}$. Henceforth, the cross section is given by

$$\sigma_i = \frac{(2\pi)^4}{4E_{p_1}E_{p_2}|v_1 - v_2|}\int \frac{d^3p_3}{(2\pi)^3 2E_{p_3}}\frac{d^3p_4}{(2\pi)^3 2E_{p_4}}\delta(p_f - p_i)|\mathcal{M}_{fi}|^2 \tag{C.16}$$

Having the matrix element $\mathcal{M}_{fi}$ we can calculate the cross section.

Since the cross section is Lorentz invariant we can consider the center-of-mass frame. In this frame $\vec{p}_1 + \vec{p}_2 = \vec{p}_3 + \vec{p}_4 = 0$ and using that $\vec{v} = \frac{\vec{p}}{E}$,

$$\sigma_i = \frac{|\mathcal{M}_{fi}|^2}{64\pi^2(E_{p_1} + E_{p_2})|\vec{p}_1|} \int \frac{d^3p_3}{E_{p_3}} \frac{d^3p_4}{E_{p_4}} \delta(p_f - p_i). \tag{C.17}$$

The integrand can be written as $\delta(p_f - p_i) = \delta(E_{p_3} + E_{p_4} - \sqrt{s})\delta(\vec{p}_3 + \vec{p}_4)$, where in the CM frame $s = (E_{p_1} + E_{p_2})^2$. Making the change of variable $w = E_{p_1} + E_{p_2}$, it results that

$$\sigma_i = \frac{|\mathcal{M}_{fi}|^2}{64\pi^2\sqrt{s}|\vec{p}_1|} \frac{|\vec{p}_3|}{\sqrt{s}} \int d\Omega(\hat{p}_3) \tag{C.18}$$

$$= \frac{|\mathcal{M}_{fi}|^2}{16\pi s} \frac{|\vec{p}_3|}{|\vec{p}_1|}. \tag{C.19}$$

Using the identity $E^2 = m^2 + |\vec{p}|^2$ and the fact that in the CM frame $E_{p_1}^2 - E_{p_2}^2 = m_1^2 - m_2^2$, we have that

$$|\vec{p}_1| = \frac{\sqrt{s(s - 2(m_1^2 + m_2^2)) + (m_1^2 - m_2^2)}}{2\sqrt{s}}, \tag{C.20}$$

$$|\vec{p}_3| = \frac{\sqrt{s(s - 2(m_3^2 + m_4^2)) + (m_3^2 - m_4^2)}}{2\sqrt{s}}. \tag{C.21}$$

Specifying for the process $\pi^+\pi^- \to \gamma\gamma$, we have that

$$\frac{|\vec{p}_3|}{|\vec{p}_1|} = \sqrt{\frac{s}{s - 4\mu^2}} \tag{C.22}$$

which leads to, multiplying by a symmetry factor $1/2$ due to the final state of two identical photons,

$$\sigma_i = \frac{|\mathcal{M}_{fi}|^2}{32\pi\sqrt{s(s - 4\mu^2)}}. \tag{C.23}$$

In the center-of-mass frame, the flux of incident particles is $|\vec{f}| = n(|\frac{\vec{p}_1}{E_{p_1}} - \frac{\vec{p}_2}{E_{p_2}}|)$, where n is the number density of the incident particles. In this frame:

$$E_{p_1} = \frac{\sqrt{s}}{2}, \tag{C.24}$$

$$|\vec{p}_1| = \frac{\sqrt{s(s - 4\mu^2)}}{2\sqrt{s}}, \tag{C.25}$$

which results in the annihilation rate per particle:

$$\Gamma_a = \frac{2}{V_{cloud}} \frac{32\pi^2\alpha^2}{32\pi s} \tag{C.26}$$

$$\approx \frac{\pi\alpha^2}{2\mu^2 V_{cloud}} \tag{C.27}$$

and so we see that this rate will depend on the mass of the black hole, $\Gamma_a = \Gamma_a(\alpha_\mu)$.

Bibliography

[1] J. Rosa, *Lie Groups and Lie Algebras in Particle Physics*.

[2] B. Carr, in *Symposium on Illuminating Dark Matter Kruen, Germany, May 13-19, 2018* (2019) arXiv:1901.07803 [astro-ph.CO] .

[3] R. Brito, V. Cardoso and P. Pani, *Superradiance*, Lect. Notes Phys. **906**, pp.1 (2015), arXiv:1501.06570 [gr-qc] .

[4] Y. B. Zel'dovich and I. D. Novikov, *The Hypothesis of Cores Retarded during Expansion and the Hot Cosmological Model*, azh **43**, 758 (1966).

[5] S. Hawking, *Gravitationally Collapsed Objects of Very Low Mass*, Monthly Notices of the Royal Astronomical Society **152**, 75 (1971), http://oup.prod.sis.lan/mnras/article-pdf/152/1/75/9360899/mnras152-0075.pdf .

[6] B. J. Carr and S. W. Hawking, *Black Holes in the Early Universe*, Monthly Notices of the Royal Astronomical Society **168**, 399 (1974), http://oup.prod.sis.lan/mnras/article-pdf/168/2/399/8079885/mnras168-0399.pdf .

[7] S. W. Hawking, *Particle Creation by Black Holes*, *Euclidean quantum gravity*, Commun. Math. Phys. **43**, 199 (1975), [,167(1975)].

[8] V. Cardoso, *Black hole bombs and explosions: from astrophysics to particle physics*, General Relativity and Gravitation **45**, 2079 (2013).

[9] R. Brito, V. Cardoso and P. Pani, *Black holes as particle detectors: evolution of superradiant instabilities*, Class. Quant. Grav. **32**, 134001 (2015), arXiv:1411.0686 [gr-qc] .

[10] R. Peccei and H. Quinn, *CP Conservation in the Presence of Pseudoparticles*, Physical Review Letters - PHYS REV LETT **38**, 1440 (1977).

[11] D. E. Gruber, J. L. Matteson, L. E. Peterson and G. V. Jung, *The spectrum of diffuse cosmic hard x-rays measured with heao-1*, Astrophys. J. **520**, 124 (1999), arXiv:astro-ph/9903492 [astro-ph] .

[12] G. Weidenspointner, *The Origin of the Cosmic Gamma-Ray Background in the COMPTEL Energy Range*, (1999).

[13] A. W. Strong, I. V. Moskalenko and O. Reimer, *A new determination of the extragalactic diffuse gamma-ray background from egret data*, Astrophys. J. **613**, 956 (2004), arXiv:astro-ph/0405441 [astro-ph] .

[14] A. Abdo, M. Ackermann, M. Ajello, W. Atwood, *et al.*, *Spectrum of the isotropic diffuse gamma-ray emission derived from first-year fermi large area telescope data*, Physical Review Letters **104**, 101101 (2010).

[15] K. Schwarzschild, *On the gravitational field of a mass point according to Einstein's theory*, Sitzungsber. Preuss. Akad. Wiss. Berlin (Math. Phys.) **1916**, 189 (1916), arXiv:physics/9905030 [physics] .

[16] P. K. Townsend, *Black holes: Lecture notes*, (1997), arXiv:gr-qc/9707012 [gr-qc] .

[17] S. W. Hawking and G. F. R. Ellis, *The Large Scale Structure of Space-Time*, Cambridge Monographs on Mathematical Physics (Cambridge University Press, 1973).

[18] M. Costa, *Teoria Quântica de Campo: Apontamentos da unidade curricular*.

[19] M. D. Schwartz, *Quantum Field Theory and the Standard Model* (Cambridge University Press, 2014).

[20] M. E. Peskin, *An introduction to quantum field theory* (CRC Press, 2018).

[21] A. Hansen and F. Ravndal, *Klein's Paradox and Its Resolution*, Physica Scripta **23**, 1036 (1981).

[22] C. A. Manogue, *The Klein paradox and superradiance*, Annals of Physics **181**, 261 (1988).

[23] J. G. Rosa, *Boosted black string bombs*, JHEP **02**, 014 (2013), arXiv:1209.4211 [hep-th] .

[24] M. Abramowitz and I. A. Stegun, *Handbook of mathematical functions with formulas, graphs, and mathematical tables*, Washington: US Govt. Print (2006).

[25] A. A. Starobinsky, *Amplification of waves reflected from a rotating "black hole"*., Sov. Phys. JETP **37**, 28 (1973), [Zh. Eksp. Teor. Fiz.64,48(1973)].

[26] H. Furuhashi and Y. Nambu, *Instability of massive scalar fields in Kerr-Newman space-time*, Prog. Theor. Phys. **112**, 983 (2004), arXiv:gr-qc/0402037 [gr-qc] .

[27] J. G. Rosa and T. W. Kephart, *Stimulated Axion Decay in Superradiant Clouds around Primordial Black Holes*, Phys. Rev. Lett. **120**, 231102 (2018), arXiv:1709.06581 [gr-qc] .

[28] S. R. Dolan, *Instability of the massive Klein-Gordon field on the Kerr spacetime*, Phys. Rev. **D76**, 084001 (2007), arXiv:0705.2880 [gr-qc] .

[29] H. Yoshino and H. Kodama, *The bosenova and axiverse*, Class. Quant. Grav. **32**, 214001 (2015), arXiv:1505.00714 [gr-qc] .

[30] H. Kodama and H. Yoshino, *Axiverse and Black Hole, Proceedings, 2011 Asia Pacific School/Workshop on Cosmology and Gravitation: Shanghai, China, February 10-14, 2011*, Int. J. Mod. Phys. Conf. Ser. **7**, 84 (2012), arXiv:1108.1365 [hep-th] .

[31] A. Arvanitaki and S. Dubovsky, *Exploring the String Axiverse with Precision Black Hole Physics*, Phys. Rev. **D83**, 044026 (2011), arXiv:1004.3558 [hep-th] .

[32] P. Pani, V. Cardoso, L. Gualtieri, E. Berti and A. Ishibashi, *Black hole bombs and photon mass bounds*, Phys. Rev. Lett. **109**, 131102 (2012), arXiv:1209.0465 [gr-qc] .

[33] P. Pani, V. Cardoso, L. Gualtieri, E. Berti and A. Ishibashi, *Perturbations of slowly rotating black holes: massive vector fields in the Kerr metric*, Phys. Rev. **D86**, 104017 (2012), arXiv:1209.0773 [gr-qc] .

[34] H. Yukawa, *On the Interaction of Elementary Particles I*, Proc. Phys. Math. Soc. Jap. **17**, 48 (1935), [Prog. Theor. Phys. Suppl.1,1(1935)].

[35] D. Griffiths, *Introduction to Elementary Particles*, Introduction to Elementary Particles by David Griffiths. Wiley, 2008. ISBN: 978-3-527-40601-2 (2008), 10.1002/9783527618460.

[36] M. Gell-Mann, in *50 years of quarks*, edited by H. Fritzsch and M. Gell-Mann (2015) pp. 1–4.

[37] M. Thomson, *Modern particle physics* (Cambridge University Press, New York, 2013).

[38] D. B. Kaplan, *lectures on Effective Field Theory*, arXiv preprint nuclth/0510023 (5).

[39] H. Sazdjian, in *EPJ Web of Conferences*, Vol. 137 (EDP Sciences, 2017) p. 02001.

[40] A. Bernstein and B. R. Holstein, *Neutral pion lifetime measurements and the QCD chiral anomaly*, Reviews of Modern Physics **85**, 49 (2013).

[41] M. Tanabashi, K. Hagiwara, K. Hikasa, K. Nakamura, *et al.* (Particle Data Group), *Review of Particle Physics*, Phys. Rev. D **98**, 030001 (2018).

[42] B. J. Carr, K. Kohri, Y. Sendouda and J. Yokoyama, *New cosmological constraints on primordial black holes*, Phys. Rev. **D81**, 104019 (2010), arXiv:0912.5297 [astro-ph.CO] .

[43] G. F. Chapline, *Cosmological effects of primordial black holes*, Nature **253**, 251 (1975).

[44] B. J. Carr, *Primordial black holes-recent developments*, arXiv preprint astro-ph/0504034 (2005).

[45] B. J. Carr, J. H. Gilbert and J. E. Lidsey, *Black hole relics and inflation: Limits on blue perturbation spectra*, Phys. Rev. **D50**, 4853 (1994), arXiv:astro-ph/9405027 [astro-ph] .

[46] J. Yokoyama, *Formation of MACHO primordial black holes in inflationary cosmology*, Astron. Astrophys. **318**, 673 (1997), arXiv:astro-ph/9509027 [astro-ph] .

[47] D. H. Lyth, *Primordial black hole formation and hybrid inflation*, arXiv preprint arXiv:1107.1681 (2011).

[48] E. Bugaev and P. Klimai, *Formation of primordial black holes from non-Gaussian perturbations produced in a waterfall transition*, Phys. Rev. **D85**, 103504 (2012), arXiv:1112.5601 [astro-ph.CO] .

[49] J. C. Niemeyer and K. Jedamzik, *Dynamics of primordial black hole formation*, Phys. Rev. **D59**, 124013 (1999), arXiv:astro-ph/9901292 [astro-ph] .

[50] J. Garcia-Bellido, A. D. Linde and D. Wands, *Density perturbations and black hole formation in hybrid inflation*, Phys. Rev. **D54**, 6040 (1996), arXiv:astro-ph/9605094 [astro-ph] .

[51] B. J. Carr and J. E. Lidsey, *Primordial black holes and generalized constraints on chaotic inflation*, Physical Review D **48**, 543 (1993).

[52] J. Rosa, *Introduction to Cosmology: Lecture Notes*.

[53] B. J. Carr, *The primordial black hole mass spectrum*, apj **201**, 1 (1975).

[54] K. Kohri, D. H. Lyth and A. Melchiorri, *Black hole formation and slow-roll inflation*, JCAP **0804**, 038 (2008), arXiv:0711.5006 [hep-ph] .

[55] T. Chiba and S. Yokoyama, *Spin distribution of primordial black holes*, Progress of Theoretical and Experimental Physics **2017** (2017).

[56] M. Mirbabayi, A. Gruzinov and J. Noreña, *Spin of Primordial Black Holes*, (2019), arXiv:1901.05963 [astro-ph.CO] .

[57] T. Harada, C.-M. Yoo, K. Kohri and K.-I. Nakao, *Spins of primordial black holes formed in the matter-dominated phase of the Universe*, Phys. Rev. **D96**, 083517 (2017), [Erratum: Phys. Rev.D99,no.6,069904(2019)], arXiv:1707.03595 [gr-qc] .

[58] A. Arbey, J. Auffinger and J. Silk, *Any extremal black holes are primordial*, arXiv preprint arXiv:1906.04196 (2019).

[59] A. Arbey, J. Auffinger and J. Silk, *Constraining primordial black hole masses with the isotropic gamma ray background*, (2019), arXiv:1906.04750 [astro-ph.CO] .

[60] J. H. MacGibbon, *Quark- and gluon-jet emission from primordial black holes. II. The emission over the black-hole lifetime*, Phys. Rev. D **44**, 376 (1991).

[61] J. H. MacGibbon, B. J. Carr and D. N. Page, *Do evaporating black holes form photospheres?*, Physical Review D **78**, 064043 (2008).

[62] B. Nayak and L. P. Singh, *Brans–Dicke Theory and Primordial Black Holes in Early Matter-Dominated Era*, International Journal of Theoretical Physics **51**, 1386 (2012).

[63] B. Carr, F. Kühnel and M. Sandstad, *Primordial black holes as dark matter*, Physical Review D **94**, 083504 (2016).

[64] C. Zhang, Q. Yu and Y. Lu, *Simulating the galaxy cluster "El Gordo" and identifying the merger configuration*, The Astrophysical Journal **813**, 129 (2015).

[65] L. Jiang, J. Wu, F. Bian, Y.-K. Chiang, *et al.*, *A giant protocluster of galaxies at redshift 5.7*, Nature Astronomy **2**, 962 (2018).

[66] R. H. Cyburt, B. D. Fields and K. A. Olive, *Primordial nucleosynthesis in light of WMAP*, Phys. Lett. **B567**, 227 (2003), arXiv:astro-ph/0302431 [astro-ph] .

[67] Y. B. Zel'Dovich, *Generation of Waves by a Rotating Body*, Soviet Journal of Experimental and Theoretical Physics Letters **14**, 180 (1971).